Environment International 146 (2021) 106240

Contents lists available at ScienceDirect

Environment International

journal homepage: www.elsevier.com/locate/envint

Effects of a human-based mixture of persistent organic pollutants on the *in vivo* exposed cerebellum and cerebellar neuronal cultures exposed *in vitro*

Hanne Friis Berntsen [a,b,*], Nur Duale [c], Cesilie Granum Bjørklund [a], Oscar Daniel Rangel-Huerta [d], Kine Dyrberg [a], Tim Hofer [e], Kirsten Eline Rakkestad [f], Gunn Østby [a], Ruth Halsne [a], Gudrun Boge [g], Ragnhild Elisabeth Paulsen [f], Oddvar Myhre [e], Erik Ropstad [a]

[a] Department of Production Animal Clinical Sciences, NMBU-School of Veterinary Science, P.O. Box 369 sentrum, N-0102 Oslo, Norway
[b] National Institute of Occupational Health, P.O. Box 5330 Majorstuen, 0304 Oslo, Norway
[c] Section of Molecular Toxicology, Norwegian Institute of Public Health, N-0403 Oslo, Norway
[d] Section of Chemistry and Toxinology, Norwegian Veterinary Institute, N-0454 Oslo, Norway
[e] Section of Toxicology and Risk Assessment, Norwegian Institute of Public Health, N-0403, Oslo, Norway
[f] Section for Pharmacology and Pharmaceutical Biosciences, Department of Pharmacy, University of Oslo, P.O. Box 1072, Blindern, NO-0316 Oslo, Norway
[g] Department of Companion Animal Clinical Sciences, NMBU-School of Veterinary Science, P.O. Box 369 sentrum, N-0102 Oslo, Norway

ARTICLE INFO

Handling editor: Marti Nadal

Keywords:
Persistent organic pollutants
Human relevant mixtures
Cerebellum
Neurodevelopment
Redox signalling
Gene expression

ABSTRACT

Exposure to persistent organic pollutants (POPs), encompassing chlorinated (Cl), brominated (Br) and perfluoroalkyl acid (PFAA) compounds is associated with adverse neurobehaviour in humans and animals, and is observed to cause adverse effects in nerve cell cultures. Most studies focus on single POPs, whereas studies on effects of complex mixtures are limited. We examined the effects of a mixture of 29 persistent compounds (Cl + Br + PFAA, named Total mixture), as well as 6 sub-mixtures on *in vitro* exposed rat cerebellar granule neurons (CGNs). Protein expression studies of cerebella from *in vivo* exposed mice offspring were also conducted. The selection of chemicals for the POP mixture was based on compounds being prominent in food, breast milk or blood from the Scandinavian human population. The Total mixture and sub-mixtures containing PFAAs caused greater toxicity in rat CGNs than the single or combined Cl/Br sub-mixtures, with significant impact on viability from 500x human blood levels. The potencies for these mixtures based on LC_{50} values were Br + PFAA mixture > Total mixture > Cl + PFAA mixture > PFAA mixture. These mixtures also accelerated induced lipid peroxidation. Protection by the competitive N-methyl-D-aspartate (NMDA) receptor antagonist 3-((*R*)-2-Carboxypiperazin-4-yl)-propyl-1-phosphonic acid (CPP) indicated involvement of the NMDA receptor in PFAA and Total mixture-, but not Cl mixture-induced toxicity. Gene-expression studies in rat CGNs using a sub-toxic and marginally toxic concentration ((0.4 nM-5.5 μM) 333x and (1 nM-8.2 μM) 500x human blood levels) of the mixtures, revealed differential expression of genes involved in apoptosis, oxidative stress, neurotransmission and cerebellar development, with more genes affected at the marginally toxic concentration. The two important neurodevelopmental markers *Pax6* and *Grin2b* were downregulated at 500x human blood levels, accompanied by decreases in PAX6 and GluN2B protein levels, in cerebellum of offspring mice from mothers exposed to the Total mixture throughout pregnancy and lactation. In rat CGNs, the glutathione peroxidase gene *Prdx6* and the regulatory transmembrane glycoprotein gene *Sirpa* were highly upregulated at both concentrations. In conclusion, our results support that early-life exposure to mixtures of POPs can cause adverse neurodevelopmental effects.

* Corresponding author at: Department of Production Animal Clinical Sciences, NMBU-School of Veterinary Science, P.O. Box 369 sentrum N-0102 Oslo, Norway.
E-mail addresses: hanne.friis.berntsen@nmbu.no, Hanne.Berntsen@stami.no (H.F. Berntsen), Nur.Duale@fhi.no (N. Duale), cesilie@permakem.no (C.G. Bjørklund), Oscar.Daniel.Rangel.Huerta@vetinst.no (O.D. Rangel-Huerta), kine.dyrberg@tine.no (K. Dyrberg), Tim.Hofer@fhi.no (T. Hofer), KirstenEline.Rakkestad@vkm.no (K.E. Rakkestad), gunn.ostby@nmbu.no (G. Østby), ruhals@ous-hf.no (R. Halsne), Gudrun.Boge@legemiddelverket.no (G. Boge), r.e.paulsen@farmasi.uio.no (R.E. Paulsen), Oddvar.Myhre@fhi.no (O. Myhre), erik.ropstad@nmbu.no (E. Ropstad).

https://doi.org/10.1016/j.envint.2020.106240
Received 4 June 2020; Received in revised form 25 September 2020; Accepted 22 October 2020
Available online 11 November 2020

1. Introduction

Persistent organic pollutants (POPs) may be defined as compounds which are potentially toxic, resistant to degradation, and tend to bioaccumulate and biomagnify in humans and animals. POPs are also subject to long range atmospheric transport (Secretariat of the Stockholm convention, 2017). Amongst the POPs there are chlorinated, brominated, and perfluorinated compounds. Whereas most chlorinated POPs were banned in the late 70′s, certain brominated and many perfluorinated compounds are still in use. Well known examples of current applications of POPs include the use of DDT as an antimalarial agent (Secretariat of the Stockholm Convention, 2019a), brominated compounds as flame retardants (Secretariat of the Stockholm convention, 2017), and perfluorinated chemicals in consumer products such as paints and inks, impregnation sprays, outdoor clothing, food wrapping papers as well as ski waxes (IVF Swerea, 2009; Kotthoff et al., 2015). Due to their persistent nature and potential for bioaccumulation, POPs may be found at measurable concentrations in tissues from humans and animals, including the brain, despite many of them being banned decades ago.

Whereas the chlorinated and brominated POPs are lipophilic and distribute mainly to lipid rich tissues such as blood lipids and adipose tissue, the perfluorinated compounds associate with proteins, and are detected at highest concentrations in the liver, kidney and blood (Karrman et al., 2006; Lau, 2012). However, all three classes of compounds may be detected in human brain samples (Dewailly et al., 1999; Maestri et al., 2006; Mitchell et al., 2012). POPs are found to cross the placenta (Li et al., 2013a; Vizcaino et al., 2014; Fisher et al., 2016) as well as being excreted in human breast milk (Karrman et al., 2007; Polder et al., 2008; Thomsen et al., 2010), resulting in potential exposure of the embryo/neonate during the sensitive perinatal period where the blood–brain-barrier may still not be completely mature. A recent study examining concentrations of perfluoroalkyl substances in 1st, 2nd and third trimester embryos and foetuses, did detect the presence of perfluorooctanesulfonic acid (PFOS) and perfluorooctanoic acid (PFOA) in samples from brain (Mamsen et al., 2019).

There are numerous published studies using single POPs or mixtures containing a few POPs reporting potential adverse effects in nerve cell cultures or effects on behaviour in animal studies (for review on organochlorine pesticides see Abreu-Villaca and Levin (2017), for polychlorinated biphenyls (PCBs) and brominated flame retardants see Kodavanti (2006), Fonnum and Mariussen (2009), Hendriks and Westerink (2015), Pessah et al. (2019) and for perfluoroalkyl acids (PFAAs) see Mariussen (2012) and Zeng et al. (2019)). However, studies using mixtures containing both chlorinated, brominated and perfluorinated compounds are scarce. Results from epidemiological studies examining neurodevelopmental effects of POP exposure are inconsistent, however prenatal exposure to PCB and DDE has been associated with poor attention in early infancy (Sagiv et al., 2008), as well as attention deficit hyperactivity disorder (ADHD)-like behaviour in childhood (Sagiv et al., 2010; Sagiv et al., 2012), whereas prenatal and postnatal exposure to polybrominated diphenyl ethers (PBDEs) has been associated with poorer attention, executive functions and hyperactivity (Roze et al., 2009; Gascon et al., 2011; Hoffman et al., 2012; Eskenazi et al., 2013; Chen et al., 2014a; Sagiv et al., 2015). Prenatal exposure to PFOS was adversely associated with gross motor development in 2 year olds (Chen et al., 2013), as well as executive function deficits in school-age children (Vuong et al., 2016). Further, prenatal exposure to PFOA and PFOS was associated with a small to moderate effect on neurodevelopment, specifically in terms of hyperactivity (Hoyer et al., 2015) and Harris et al. (2018) found associations between prenatal and childhood per- and polyfluoroalkyl substance (PFAS) exposure and lower childhood visual motor abilities. A recent study examining the effects of 27 POPs in a cohort of Norwegian children found an association between early-life exposure to β-HCH and PFOS and ADHD (Lenters et al., 2019).

Although plausible relationships and outcomes of POP exposure may be determined by epidemiological or human sampling studies, *in vivo* and *in vitro* studies are important for the establishment of potential mechanisms of action that may have an impact on neurodevelopment. Whereas many of the previously published studies on POPs focus on single chemicals, we are in real life exposed simultaneously to a large number of compounds. These compounds may potentially exert additive, synergistic or also antagonistic effects on a specific target when combined. In the present study, we thus used a human-based mixture of 29 chlorinated, brominated and perfluorinated POPs (called Total mixture) or sub-mixtures thereof, for the investigation of different endpoints after *in vivo* and *in vitro* exposure. Most of the compounds included in the mixtures are defined as POPs under the Stockholm Convention on Persistent Organic Pollutants, with the exception of the perfluorinated compounds perfluorohexanesulfonic acid (PFHxS), perfluorononanoic acid (PFNA), perfluorodecanoic acid (PFDA), and perfluoroundecanoic acid (PFUnDA). Whereas PFHxS is currently proposed for listing (Secretariat of the Stockholm Convention, 2019b), PFNA, PFDA and PFUnDA have also been found to have long elimination half-lives in humans (Freberg et al., 2010; Nilsson et al., 2010). For the *in vivo* studies, the relationship between the various compounds in the mixture were based upon human estimated daily intake values, whereas for the *in vitro* studies the concentrations were based on levels of POPs measured in human blood (for further details on the mixtures see section 2.2, and Berntsen et al., 2017a).

In the present study we used *in vitro* cultures of cerebellar granule neurons (CGNs) and cerebellum from *in vivo* exposed mice for the study of exposure to the mixtures of POPs. Cerebellum as a model has the advantage that it is evolutionary conserved across species. It has functions in motor control, but also in cognition, learning and memory, speech production, execution of tasks, and social and emotional behaviour (Schmahmann, 2010). While data suggest cerebellar involvement in several neuropsychiatric disorders, the most significant evidence exist for ADHD and autism spectrum disorders (ASD) (Schmahmann, 2010), which are both linked to exposure to POPs. *In vitro* cultures of CGNs are suitable for studies of glutamatergic nerve cell function. As they may be cultured to a high purity with little glial cell contamination (<3%, (Nicoletti et al., 1986)) they are also well suited for the study of effects on genetic markers located specifically to neurons.

During cerebellar development, cerebellar post-mitotic granule neurons migrate from the external granule layer (EGL) to the internal granule layer (IGL) where they differentiate into mature neurons (Rakic, 1971). *Pax6* (a paired box transcription factor) has been identified as important in the development of various structures of the central nervous system, including the cerebellum (Yeung et al., 2016). It is expressed in granule cells throughout their differentiation and migration and is expressed at higher levels in the EGL than in the IGL (Yamasaki et al., 2001). Loss of *Pax6* in mutant mice causes a disruption of the correct migration of granule cells as well as the proper organisation of post-mitotic cells. In cerebellar explant cultures from embryonic mice, neurite outgrowth and neuronal migration is affected (Engelkamp et al., 1999; Yamasaki et al., 2001). Clinically, mutations in *Pax6* have been linked to autism (Maekawa et al., 2009). It is well known that the N-methyl-D-aspartate receptor (NMDA-R) is permeant to Ca^{2+}, which mediates many of the functions of NMDA-R activity, including synaptic modification, learning and memory, activity-dependent development, and neuroprotective/homeostatic signalling (Bell and Hardingham, 2011; Paoletti et al., 2013; Wyllie et al., 2013). The *Grin2b* gene, encoding the GluN2B subunit of the NMDA-R, has been recognised to play an important role in synaptogenesis and plasticity (Akashi et al., 2009; Espinosa et al., 2009; Paoletti et al., 2013). Like *Pax6*, *Grin2b* is expressed during early development, and is important during the migration of neurons from the EGL to the IGL (Llansola et al., 2005; Mancini and Atchison, 2007). Loss of function of the gene may result in developmental delay (Mishra et al., 2016). In addition, *Grin2b* variants have been associated with ASD, mental retardation and schizophrenia

(Endele et al., 2010; Pan et al., 2015). We have previously observed that PAX-6 and GluN2B are important markers for the differentiation of CGNs from mouse and chicken, and that their expression may be altered by xenobiotic exposure (Mathisen et al., 2013; Fjelldal et al., 2019).

POPs from both the chlorinated, brominated and perfluorinated groups of compounds have previously been observed to induce toxicity in cultures of CGNs from rat (Tan et al., 2004; Kodavanti et al., 2005; Berntsen et al., 2017b, 2018). In the present study our aim was to assess the *in vitro* toxicity in rat CGNs of the Total POP mixture containing both chlorinated, brominated and perfluorinated compounds , and to compare it to the toxicity of one or several of six sub-mixtures containing only one or two groups of chemicals. Based on previously reported effects on end-points in studies using single compounds from the three chemical groups (Mariussen et al., 2002; Reistad et al., 2006, 2007; Berntsen et al., 2017b, 2018) we specifically aimed to investigate whether lipid peroxidation, reactive oxygen species (ROS) production and involvement of the NMDA-R could be observed after exposure to the mixtures. Further, we wanted to assess how a selected panel of genes, including genes involved in apoptosis, redox signalling, genes encoding the oestrogen receptor, genes related to neurotransmission, and genes important during cerebellar development (*Pax6* and *Grin2b*) were affected by exposure to a sub-toxic (333x), and a marginally toxic (500x) concentration of the mixtures. Finally, we sought to verify whether effects on PAX6 and GluN2B protein levels could be observed in the cerebellum from offspring mice (sacrificed for use in a separate study), from mothers exposed throughout pregnancy and lactation to the same 29 compounds as found in the Total *in vitro* mixture.

2. Materials and methods

2.1. Chemicals and reagents

Anti-NMDAR GluN2B antibody (ab65783) was from Abcam (Cambridge, UK). Goat anti-mouse (H + L)-HRP conjugate was obtained from Bio-Rad (Hercules, California, US). The chlorinated compounds and PBDE congeners used for the mixtures were purchased from Chiron AS (Trondheim, Norway). Basal medium Eagle (BME), C_{11}-BODIPY, 2′,7′-dichlorodihydrofluorescein diacetate (DCFH-DA), heat inactivated foetal bovine serum (FBS), Glutamax-I supplement – 200 mM, Hanks' Balanced Salt Solution (HBSS) – 10X, HEPES buffer – 1 M and penicillin–streptomycin 100 IU/ml penicillin and 100 μg/ml streptomycin were obtained from GIBCO/Invitrogen, Norway. KAPA SYBR® FAST qPCR Master Mix (2X) was obtained from Kapa Biosystems, (London, UK). Anti-PAX6-antibody (ab2237), sodium orthovanadate (Na_3VO_4), sodium selenite (selenite, ≥ 98%), 3,3′,5-triiodo-L-thyronine sodium salt (T3, ≥ 95.0%), trypan blue (TB), Luminata Western Classico and Luminata Western Crescendo came from Merck Millipore (Temecula, CA, USA). H_2O_2 was purchased from Norsk Medisinaldepot AS, Oslo, Norway. Donkey anti-rabbit horseradish peroxidase (HRP) conjugated secondary antibody and tridecafluorohexane-1-sulfonic acid potassium salt (PFHxS, > 98%) came from Santa Cruz Biotechnology (Santa Cruz, CA, USA). Albumin from bovine serum (BSA, ≥ 96%), cumene hydroperoxide (CumOOH) – 6 M, cytosine β-D-arabinofuranoside (ARA-C), deoxyribonuclease I from bovine pancreas (DNAse), dimethyl sulfoxide (DMSO, ≥ 99.9%), hexabromocyclododecane (HBCD), holo-transferrin human (transferrin, ≥ 97.0%), leupeptin hydrochloride (≥ 90%), L-glutamine (glutamine, 99.0–101.0%), mouse monoclonal anti-β-ACTIN antibody, pepstatin A (≥ 90%), the perfluorinated compounds used individually/for the mixtures (with the exception of PFHxS), phenylmethylsulfonyl fluoride (PMSF, 0.1 M in ethanol), poly-L-lysine hydrobromide – M_w > 70000, putrescine dihydrochloride (putrescine, ≥ 97%), 3-(4,5-dimethylthiazol-2-yl)-2,5-diphenyl tetrazolium bromide (MTT), trypsin type I from bovine pancreas and trypsin inhibitor from glycine max (soybean) type I-S were purchased from Sigma-Aldrich (St. Louis, MO, USA). High Capacity cDNA Reverse Transcription Kit and Pierce® BCA Protein Assay Kit was from Thermo Scientific (Rockford, IL, USA). 3-((*R*)-2-Carboxypiperazin-4-yl)-propyl-1-phosphonic acid (CPP, ≥ 98%) was purchased from Tocris Biosciences (Bristol, UK). Quick-RNA™ MiniPrep Plus was purchased from Zymo Research (Irvine, CA, USA). All other chemicals and reagents used were obtained from standard commercial suppliers. Stock solutions of C_{11}-BODIPY and DCFH-DA, were prepared by dissolution in DMSO. The stocks of the mixtures and PFOS were prepared by dissolution in DMSO and were frozen and thawed between experiments to ensure use of the same stock solutions.

2.2. Mixtures

The mixtures of POPs used in the present study were designed and prepared at the Norwegian University of Life Sciences as described in Berntsen et al. (2017a), and more details on the design and selection of compounds may be found in the main article and supplementary material. In brief, a literature review was conducted on the most recent Scandinavian studies reporting levels of POPs in blood, breast milk and/or food prior to 2012, and compounds occurring at the highest levels selected for incorporation into the mixtures. The mixtures were designed to be used in various *in vitro* and *in vivo* models.

2.2.1. Mixtures used in vitro

For *in vitro* studies the concentrations of chemicals in the mixtures were based on Scandinavian human blood levels. The stocks used in the present study had a concentration of 1000000 times blood levels and were diluted down to relevant concentrations for use in the different experiments.

In brief 7 different mixtures were composed; the Cl mixture containing chlorinated compounds (PCB 28,52,101,118,138,153 and 180, *p,p'*-dichlorodiphenyldichloroethylene (DDE), hexachlorobenzene (HCB), α-chlordane, oxychlordane, *trans*-nonachlor, α-hexachlorocyclohexane (HCH), β-HCH, γ-HCH (lindane) and dieldrin), the Br mixture containing brominated compounds (PBDEs: BDE-47,-99,-100,-153,-154 and -209 as well as HBCD), the PFAA mixture containing perfluorinated compounds (perfluorohexanesulfonic acid potassium salt (PFHxS), perfluorooctanesulfonic acid potassium salt (PFOS), PFOA, perfluorononanoic acid (PFNA), perfluorodecanoic acid (PFDA) and perfluoroundecanoic acid (PFUnDA)), the Cl + Br mixture containing chlorinated and brominated compounds, the Cl + PFAA mixture containing chlorinated and perfluorinated compounds, the Br + PFAA mixture containing brominated and perfluorinated compounds, and the Total mixture containing all the three chemical groups. Chemical levels in the 7 mixtures were measured and verified as described in (Berntsen et al., 2017a). The concentrations of the various compounds at x-times blood levels for the different exposures used are presented in Table 1 in μM and μg/ml concentrations. Due to little deviations between the measured compounds in the different stocks used, only the values for the Total mixture are presented, being representative for all stocks.

2.2.2. Mixtures administered in vivo

For animal exposure a mixture containing the same compounds as used in the *in vitro* mixture was composed and incorporated into animal feed. However, combinations of concentrations for the different compounds were based on average Scandinavian estimated daily intake (EDI) values for a 70 kg person. The average human EDIs calculated were adjusted to mice assuming a mean body weight for the mice of 25 g, and a feed intake of 3 g feed/day (Supplementary Table S1) (Berntsen et al., 2017a). Four different diets were used for animals in the present study: one control diet containing evaporated solvents (Control), a low dose feed containing POPs at 5000x EDI (Low POPs) a high dose feed containing POPs at 100000x EDI (High POPs) and a reference feed containing only corn oil. Due to economic constraints only two POP doses were included in addition to the control feed. When doses were selected these were based on the need for intended exposures to be distinguishable from potential background exposure in the feed. The

Table 1
Mixture-concentrations of persistent organic pollutants (POPs) used for *in vitro* exposure of cerebellar granule cells.

Compounds	Exposures – times blood levels – μM							Exposures – times blood levels – μg/ml						
	250x	333x	500x	1000x	2000x	3000x	4000x	250x	333x	500x	1000x	2000x	3000x	4000x
Chlorinated compounds														
PCB 28	0.008	0.010	0.015	0.031	0.062	0.093	0.123	0.002	0.003	0.004	0.008	0.016	0.024	0.032
PCB 52	0.006	0.007	0.011	0.022	0.045	0.067	0.089	0.002	0.002	0.003	0.007	0.013	0.020	0.026
PCB 101	0.006	0.009	0.013	0.026	0.052	0.078	0.104	0.002	0.003	0.004	0.008	0.017	0.025	0.034
PCB 118	0.033	0.044	0.065	0.131	0.261	0.392	0.523	0.011	0.014	0.021	0.043	0.085	0.128	0.171
PCB 138	0.112	0.150	0.224	0.449	0.898	1.347	1.796	0.041	0.054	0.081	0.162	0.324	0.486	0.648
PCB 153	0.182	0.243	0.364	0.729	1.457	2.186	2.914	0.066	0.088	0.131	0.263	0.526	0.789	1.052
PCB 180	0.094	0.126	0.189	0.378	0.756	1.134	1.512	0.037	0.050	0.075	0.149	0.299	0.448	0.598
p,p'-DDE	0.272	0.363	0.544	1.089	2.178	3.267	4.356	0.087	0.115	0.173	0.346	0.693	1.039	1.385
HCB	0.059	0.078	0.118	0.235	0.470	0.706	0.941	0.017	0.022	0.033	0.067	0.134	0.201	0.268
α - chlordane	0.007	0.010	0.015	0.030	0.059	0.089	0.118	0.003	0.004	0.006	0.012	0.024	0.036	0.048
oxy - chlordane	0.008	0.011	0.016	0.033	0.065	0.098	0.131	0.003	0.005	0.007	0.014	0.028	0.042	0.055
trans-nonachlor	0.025	0.033	0.050	0.099	0.198	0.297	0.396	0.011	0.015	0.022	0.044	0.088	0.132	0.176
α-HCH	0.005	0.006	0.009	0.018	0.036	0.054	0.072	0.001	0.002	0.003	0.005	0.011	0.016	0.021
β-HCH	0.019	0.025	0.038	0.076	0.152	0.228	0.304	0.006	0.007	0.011	0.022	0.044	0.066	0.088
γ-HCH (Lindane)	0.005	0.006	0.009	0.019	0.038	0.057	0.076	0.001	0.002	0.003	0.006	0.011	0.017	0.022
Dieldrin	0.016	0.021	0.031	0.062	0.125	0.187	0.250	0.006	0.008	0.012	0.024	0.048	0.071	0.095
Brominated compounds														
BDE-47	0.004	0.005	0.007	0.014	0.028	0.042	0.056	0.002	0.002	0.003	0.007	0.014	0.020	0.027
BDE-99	0.002	0.002	0.003	0.006	0.013	0.019	0.025	0.001	0.001	0.002	0.004	0.007	0.011	0.014
BDE-100	0.001	0.001	0.002	0.004	0.007	0.011	0.014	0.001	0.001	0.001	0.002	0.004	0.006	0.008
BDE-153	0.0003	0.0004	0.001	0.001	0.002	0.004	0.005	0.0002	0.0003	0.0004	0.001	0.002	0.002	0.003
BDE-154	0.0005	0.001	0.001	0.002	0.004	0.006	0.008	0.0003	0.0004	0.001	0.001	0.003	0.004	0.005
BDE-209	0.002	0.003	0.005	0.009	0.019	0.028	0.037	0.002	0.003	0.004	0.009	0.018	0.027	0.036
HBCD	0.016	0.022	0.033	0.065	0.131	0.196	0.262	0.011	0.014	0.021	0.042	0.084	0.126	0.168
Perfluorinated compounds														
PFHxS	1.728	2.301	3.455	6.911	13.822	20.733	27.644	0.757	1.008	1.514	3.028	6.057	9.085	12.113
PFOS	4.092	5.450	8.183	16.367	32.733	49.100	65.467	2.202	2.933	4.404	8.809	17.618	26.427	35.236
PFOA	1.673	2.228	3.345	6.690	13.381	20.071	26.761	0.693	0.922	1.385	2.770	5.540	8.311	11.081
PFNA	0.435	0.579	0.869	1.738	3.477	5.215	6.953	0.202	0.269	0.403	0.807	1.613	2.420	3.227
PFDA	0.166	0.221	0.332	0.664	1.328	1.992	2.655	0.085	0.114	0.171	0.341	0.683	1.024	1.365
PFUnDA	0.069	0.092	0.138	0.276	0.552	0.828	1.103	0.039	0.052	0.078	0.156	0.312	0.468	0.624

Note. Cells were in the different experiments exposed to one or several of the concentrations 250x, 333x, 500x, 1000x, 2000x, 3000x and 4000x the values found in Scandinavian human blood (Berntsen et al., 2017a) (x = times). Due to little deviations between the measured concentrations in the mixtures used, only the measured stock values for the Total mixture are presented. The exposure concentrations of the different compounds used are in μM and corresponding μg/ml values.

feed company, which incorporated the mixtures into pelleted feed, allowed for a substantial background level of POPs in their diets, thus the 5000xEDI dose was chosen to provide feed concentrations at the same level, or for some compounds, lower than the company's maximum allowed feed contamination level. As there was a need to clearly be able to distinguish the two exposure groups, and to make it more likely to achieve an effect of a mixed exposure, a second dose 20 times higher than for the low exposure feed, 100000x EDI, was selected as the high dose. As described in Berntsen et al. (2017), the 100000x EDI concentrations for the individual mixture compounds were mainly lower than the no observed adverse effect levels (NOAEL), where such values were available. Some of the individual 5000x EDI concentrations were close to, while most exceeded the established tolerable daily intake (TDI) values used by regulatory agencies in Europe, US, and Canada (ATSDR, 2005; EFSA 2005, 2008; EPA 2008; Health-Canada 2007). The estimated daily exposure doses for the individual compounds in the two exposure groups are presented in Supplementary Table S1, but the range for the compounds in the Low POPs group was: chlorinated compounds – 0.7–14.4 μg/kg/day, brominated compounds – 0.15–7.5 μg/kg/day and perfluorinated compounds – 0.09–2.2 μg/kg/day, whereas it in the High POPs group was: chlorinated compounds – 14–287 μg/kg/day, brominated compounds – 3–150 μg/kg/day and perfluorinated compounds – 1.7–44 μg/kg/day.

2.3. Laboratory animals

The rat and mice studies described in the present publication were carried out at the Animal Laboratory Unit at the Section of Experimental Biomedicine, Norwegian University of Life Sciences, whereas the treatments of chicken embryos were conducted at the Section for Pharmacology and Pharmaceutical Biosciences, Department of Pharmacy, University of Oslo. All procedures were in accordance with the Norwegian Animal Welfare Act and the Directive 2010/63/EU of the European Parliament and of the Council on the protection of animals used for scientific purposes. Efforts were made to minimise animal suffering and to reduce the number of animals used.

2.3.1. Rat pups for the isolation of CGNs

For each isolation of cells, mixed-sex litters of 10 Wistar rat pups were obtained at 8 days of age from Taconic, Denmark. The pups were euthanised, without prior use of anaesthesia, by decapitation on the day of arrival.

2.3.2. CD-1 mice for in vivo exposure

Twenty timed-pregnant CD-1 mice (F0) were obtained from Charles River Laboratories (Raleigh, NC). After weaning at 3 weeks of age, F1 females were randomly assigned into one of the three groups: Control mothers (n = 29), Low POP mothers (n = 27), and High POP mothers (n = 23), and fed with control, low exposure, and high exposure diet *ad libitum,* respectively. Animals were exposed from weaning, throughout mating, gestation, and lactation, until necropsy. At 10 weeks of age, F1 dams were mated with in-house bred CD-1 males. The resulting offspring (F2) from the exposed dams were only exposed to POPs (6 weeks) via the placenta, through suckling and by nibbling on their mothers' feed before weaning. After weaning, pups were given the reference diet, with no added POPs or solvents. During exposure animals were housed in closed type III IVC-cages (Allentown Inc, PN, USA), to reduce the exposure of personnel and to minimise the risk of cross-contamination between exposure groups. All cages contained standard aspen bedding, red polycarbonate houses and cellulose nesting material

(Scanbur BK, Karlslunde, Denmark). Water and feed were available *ad libitum*. Cages, bedding, nesting material and water bottles were changed weekly. The animal room was on a 12:12 light-dark cycle, with a room temperature of 21 ± 2°C and 45 ± 5% relative humidity. Female pups from the three groups; Control, Low POPs and High POPs were sacrificed at 7 days, 3, 6 and 9 weeks of age to use in a separate project, and the cerebella removed for western blot studies from 9 animals from each group at each time-point. Although levels of POPs were not measured in the pups in our study, pooled plasma samples (from 36 animals in each group) were obtained at 9–10 weeks of age in another study from hybrid 129:C57BL/6 pups. These pups were exposed to the same mixtures via their mothers for the same time-period as in the present study, as described in Hudecova et al. (2018). In the low dose group the chlorinated compounds were detected in the range 0.6-58x human blood levels, perfluorinated compounds at 1-56x human blood levels, and BDE-100, the only detected brominated compound at 45x human blood levels, when compared to average Scandinavian blood levels as calculated in Berntsen et al. (2017a); (Hudecova et al., 2018). Levels of POPs in the high dose group ranged from 3-701x human values for the chlorinated compounds, 22-1016x human blood levels for the perfluorinated compounds and 110-976x human levels for the three brominated compounds detected.

2.3.3. Chicken embryos for in ovo exposure and isolation of CGNs

For experiments using cerebella from chicken embryos, eggs from chicken (*Gallus gallus*) from different batches were obtained from Samvirkekylling (Våler, Norway), and incubated in an OvaEasy 380 Advance EXII incubator (Brinsea, Weston-super-Mare, UK) at 37.5 °C and 45% relative humidity until embryonic day (ED)17. To make sure that only eggs with live embryos were used for cell isolation or *in ovo* experiments, spontaneous movements by the embryo were confirmed by light transillumination of the egg with a LED lamp (Brinsea). Prior to hatching and decapitation of embryos, the eggs were put on crushed ice for 7 min.

2.4. Isolation of CGNs and in vivo exposed cerebellum

2.4.1. Isolation of rat CGNs

Primary cultures of post-mitotic CGNs from rat pups at postnatal day (PND) 8, were prepared as described in Berntsen et al. (2013), with modifications from Mariussen et al. (2002), based on the procedures originally described in Gallo et al. (1982) and Schousboe et al. (1989). Cells from each isolation were diluted to an approximate concentration of 1–1.2 × 10^6 cells/ml in BME supplemented with 10% heat-inactivated FBS, 2.5 mM Glutamax, 100 IU/ml penicillin + 100 μg/ml streptomycin, 25 mM KCl and 1% glucose (supplemented BME), and transferred (0.5 ml cells/well) to 24 well poly-L-lysine treated cell culture plates (Thermo Scientific™, Nunc™) for viability experiments involving the 7 mixtures, as well as mechanistic studies on NMDA-R involvement and gene expression studies. As exposures performed in the lipid peroxidation as well as ROS production studies were conducted on 96 well plates, for the 4 h MTT assessment related to these experiments, cells were seeded (125 μl cells/well) in 96-well microplates (Thermo Scientific™, Nunc™, MicroWell™). For the assessment of ROS production as well as lipid peroxidation, cells were seeded (125 μl cells/well) on poly-L-lysine treated black, flat, clear bottom, 96-well plates (Corning®, Costar®). The cytostatic drug ARA-C was added to all plates after 24 h - at day 1 *in vitro* (DIV), giving a concentration of 10.3 μM in the cell medium, to prevent the replication of non-neuronal cells. For the exposure of cells at DIV 0, 2x the normal concentration of cells (2–2.4 × 10^6 cells/ml in supplemented BME were seeded (0.5 ml cells/well) followed by 2x the desired final concentration of toxicants/DMSO in the same medium (0.5 ml/well), giving a concentration of 1x for the relevant toxicant/well. The cytostatic drug ARA-C was added as normal at DIV 1. After addition of ARA-C cells were left undisturbed in a CO_2 incubator at 36 °C and 5% CO_2 until DIV 7 or 8, when exposures were carried out, or in the case of cells exposed at DIV 0, until DIV 8, when the MTT assay was conducted. For all chemical treatments (with the exception of cells exposed at DIV 0) and assays conducted in the present study, cells were exposed to toxicants in the absence of FBS.

Although cultures consisting mainly of granule cells was confirmed by phase contrast microscopy, the specific percentage of remaining glial cells was not specifically assessed by staining in the present study. This has however been extensively reported by others, and primary cultures of CGNs may at DIV 8 typically be found to contain around 97% neuronal cells when the cytostatic drug ARA-C is added to the culture medium at DIV 1, as in the present study. 5% of the cells will be GABAergic basket or Golgi neurons, whereas the number of astrocytes would be < 3% (Nicoletti et al., 1986; Perez-Gomez et al., 2004).

2.4.2. Isolation of CGNs and in ovo exposed cerebellum from chicken at ED 17

CGNs were isolated from chicken embryos at ED17 as described in Jacobs et al. (2006). Cells were diluted to a concentration of 1.9 × 10^6 cells/ml in BME, supplemented with 10% heat-inactivated horse serum, 2 mM glutamine, 100 nM insulin, 100 IU/ml penicillin + 100 μg/ml streptomycin and 25 mM KCl, and transferred to 3.5 cm poly-L-lysine treated cell culture dishes (Nunc, 1 ml cells/dish). After 24 h incubation at 37 °C and 5% CO_2 the medium was at DIV 1 replaced with serum-free BME containing 2 mM glutamine, 25 μg/ml insulin, 100 IU/ml penicillin + 100 μg/ml streptomycin, 100 μg/ml transferrin, 9.6 μg/ml putrescine, 1 nM T3, 30 nM selenite and 25 mM KCl (1 ml/dish). Cells were subsequently incubated for 24 h, before exposure with 10 and 100 μM PFOS or 0.2% DMSO in serum-free medium, at DIV 2, for 24 h, and assessment of cell viability with the trypan blue (TB) exclusion assay. For *in ovo* exposure of eggs for GluN2B expression studies in cerebellum, eggs were injected at ED14 with 1 mM PFOS in 50 μl 1% DMSO in 0.9% saline onto the chorioallantoic membrane as described in Austdal et al. (2016) after transillumination to avoid blood vessels, wiping of injection area with ethanol, and perforation of the eggshell with a 27G needle. Eggs were subsequently incubated for 72 h at 38 °C. At ED17 cerebellum was removed and homogenised for western blot analysis.

2.4.3. Isolation of cerebellum from in vivo exposed mice

Cerebella were isolated from control mice, or mice from the Low POPs and High POPs groups on day 7, week 3, 6, or 9 after birth. The scull was opened along the cranial sutures to expose the cerebellum which was then detached from the brain stem. Following dissection meninges were removed with forceps and entire cerebella were placed in cryo tubes. Cerebellar tissue for western blot analysis was frozen at −196°C with liquid N_2.

2.5. Exposure of cells and assessment of cell viability

2.5.1. Exposure of rat CGNs and assessment of viability with the MTT assay

For the assessment of cell viability after 24 h exposure to the seven mixtures, rat CGNs were at DIV 8 exposed to concentrations 250x, 500x, 1000x, 2000x, 3000x and 4000x human blood levels for the different mixtures, in BME (0.5 ml/well) supplemented with 2.5 mM Glutamax, 100 IU/ml penicillin + 100 μg/ml streptomycin, 25 mM KCl and 1% glucose, without FBS, before viability was assessed with the MTT assay (n = 4 independent experiments, each from a separate cell isolation, with each condition tested in triplicate on the same plate per experiment). The assay was performed as described in Berntsen et al. (2013) with slight modifications, and dual wavelength absorbance measurements in 96-well plates were performed at 570 and 690 nm in a VICTOR3 multilabel reader (PerkinElmer, Inc. Waltham, MA, USA). In brief 250 μl MTT was used for each well of the 24 well plates and formazan dissolved in 250 μl DMSO before transfer of 100 μl formazan solution to a separate plate as previously described (Berntsen et al., 2013). For the exposures conducted in 96 well plates, medium was removed, and replaced with 100 μl medium including toxicants. Subsequently, this medium was replaced with 100 μl 0.5 mg/ml MTT

solution, which was left for 1 h before removal of the MTT and addition of 100 μl DMSO. The 96 well plates were read directly without the transferal of dissolved formazan salt solution to another plate. Exposures in the viability experiments were conducted in triplicate wells, and an average value calculated for each experiment. In each experiment a relevant DMSO control was included as well as an unexposed medium control. The calculated mean optic density values for each treatment was expressed as % of the mean values for the relevant DMSO control from the same experiment (set to 100%) as expression of viability. DMSO controls with concentrations of DMSO from 0.2 to 0.8 % were included in the viability experiments to reflect DMSO concentrations at the highest tested concentrations of the mixtures, however no effects on viability were observed for any of the tested DMSO concentrations.

As CGNs grown in 96-well plates were exposed at DIV 7 to the 7 mixtures for up to 5 h in the lipid peroxidation assay, cells grown in the same kind of plates were exposed to the 1000x human blood levels concentration (the highest tested concentration in the lipid peroxidation assay) of six of the mixtures for 5 h, before cell viability was assessed with the MTT assay (n = 3, each from a separate cell isolation, with each condition tested in triplicate on the same plate per experiment). The Br mixture was not included in this assessment due to lack of any effects on viability after 24 h exposure.

To assess effects of the mixtures on viability in CGNs at a different stage of development, cells were also exposed for 8 days to two concentrations of the seven mixtures from the time of isolation (DIV 0, n = 4 independent experiments, each from a separate cell isolation, with each condition tested in triplicate on the same plate per experiment) until DIV 8 when the MTT assay was conducted. Concentrations of 500 and 1000x were chosen for this exposure due to the induction of toxicity for most of the mixtures at these concentrations when cells were exposed at DIV 8.

2.5.2. Exposures of chicken CGNs to PFOS, and assessment of viability with the TB assay

Cell viability in chicken CGNs was assessed with the TB exclusion assay after 24 h exposure to 10 and 100 μM PFOS (n = 3). 250 μl of 1% TB solution was added to each dish/ml medium, incubated for 30 min at 37 °C and 5% CO_2 before removal of the liquid, and counting of live (white) and dead (blue) cells in 3–4 areas of each dish, resulting in a total count of 100 cells per/dish.

2.6. Mechanistic studies on NMDA-R involvement in mixture-induced cell death

For mechanistic cell-death studies of mixture-induced effects on the NMDA-receptor, the single chlorinated and perfluorinated mixtures, as well as the Total mixture were selected. The Br mixture was not included in the mechanistic studies, as no effects on cell viability were observed at the tested concentrations. Mixture concentrations giving some toxicity in the concentration–response studies were chosen. Cell viability was therefore screened after exposure of cells to 3000x blood levels of the Cl mixture or 1000x blood levels of the PFAA and Total mixtures alone or in conjunction with 10 μM of the competitive NMDA-R antagonist CPP for 24 h (n = 3). The effects of CPP on cells alone was not included in the experiments, as this was previously studied and reported as not significant for the same batch of CPP and from CGNs isolated in the same laboratory (Berntsen et al., 2018).

2.7. ROS production and lipid peroxidation

2.7.1. ROS production in rat CGNs after acute and 24 h mixture exposure assessed with the DCFH-DA assay

For the assessment of the production of ROS in CGNs after acute exposure to the various mixtures, cells from triplicate wells were at DIV 7 exposed to 1000 and 2000x human blood levels of all the seven mixtures, in addition to 4000x human blood levels of the Cl, PFAA, Cl + PFAA, Br + PFAA and Total mixtures or 1 mM H_2O_2 (positive control) in supplemented HBSS buffer (pH 7.4) (containing 20 mM HEPES, 4.17 mM $NaHCO_3$, 5 mM glucose and 25 mM KCl). Exposures were carried out for 1 h, during which ROS production was assessed with the DCFH-DA fluorescence assay, from now referred to as the DCF assay. DCFH may be oxidised to the fluorescent DCF when ROS such as $ONOO^-$, $^{\bullet}OH$ and H_2O_2 are present (Myhre et al., 2003). All experiments included an unexposed buffer control as well as a DMSO control (0.1%). A mean value was calculated for each experiment, and each experiment repeated three times in individual cell isolates (n = 3). In brief, the medium from each well of the 96 well plate was rapidly removed with a multichannel pipette, and carefully replaced with 250 μl/well of a 5 μM solution of DCFH-DA in HBSS buffer. Cells were subsequently incubated in the dark for 20 min at 36 °C and 5% CO_2, before replacement of the DCFH-DA solution with 250 μl/well of the various mixture solutions in HBSS buffer, and fluorescence readings were initiated immediately using a CLARIOstar® microplate reader (BMG Labtech, Ortenberg, BW, Germany) at room temperature. The area under the curve (AUC) was calculated for each well, and the mean values for triplicate wells in each experiment were expressed as fluorescence relative to the DMSO control (set to a relative fluorescence value of 100). In addition to measurements of ROS production after acute exposure, CGNs were exposed to 500 and 1000x human blood levels of the seven mixtures, 2000x of the Br, Cl and Cl + PFAA mixtures, or 0.1% DMSO in supplemented BME without FBS, or BME only for 24 h, before measurements of ROS. Incubation with DCFH-DA was performed as described above, after removal of the mixture solutions from respective wells. After removal of DCFH-DA, supplemented buffer was added to all wells except for three wells, where the positive control H_2O_2 was added. Fluorescence readings were thereafter initiated immediately and continued for 1 h. Each exposure was performed in triplicate wells, and each experiment repeated three times in different cell isolates (n = 3).

2.7.2. Assessment of cellular lipid peroxidation in rat CGNs

For the assessment of lipid peroxidation using the probe C_{11}-BODIPY, cells from triplicate wells were at DIV 7 exposed to 2 concentrations of the seven mixtures, 500x (with the exception of the Br mixture) or 1000x blood levels, 0.1% DMSO or supplemented buffer only, in the presence and absence of the lipid peroxidation-inducer cumene hydroperoxide (cumOOH) (n = 3). The method used in the present study was based on the cellular lipid peroxidation antioxidant assay (CLPAA) as described in Hofer et al. (2014) with modifications described in Berntsen et al. (2017b). The CLPAA assay is based on the oxidation of the cell membrane soluble and oxidation sensitive probe C_{11}-BODIPY (which emits natural red fluorescence) by free radicals, to green fluorescent C_{11}-BODIPY oxidation products. The amount of two green fluorescent molecules created by free radical attack of C_{11}-BODIPY correlates with the amount of lipid peroxidation, taking place (Hofer et al., 2014). For assessment of effects of antioxidants, lipid peroxidation can be induced with addition of cumOOH (Hofer et al., 2014). In the present study we used cumOOH as an inducer of lipid peroxidation to see whether the mixtures were capable of accelerating lipid peroxidation. As inflammation produces oxidants that may initiate lipid peroxidation, we wanted to test how the mixtures behave under on-going low-grade lipid peroxidation which can partly resemble inflammation. In addition, we assessed whether the mixtures on their own were able to influence the background lipid peroxidation rate in CGNs. Briefly medium covering cells was removed from each well of the 96-well plate and replaced with 100 μl/well of C_{11}-BODIPY (5 μM) in supplemented HBSS. The plate was subsequently incubated for 30 min in the dark at 36 °C and 5% CO_2, before the C_{11}-BODIPY solution was removed, wells washed once with 100 μl HBSS, and replaced with 200 μl of the mixtures in supplemented HBSS buffer or supplemented HBSS with cumOOH (50 μM). The plate was read immediately in a CLARIOstar® microplate reader (BMG Labtech, Ortenberg, BW, Germany) at 37 °C. Readings were continued for up to 1 h 30 min in the presence of cumOOH and up to 5 h in its absence. The increase in the green fluorescent C_{11}-BODIPY oxidation products

reflects the rate of lipid peroxidation in cellular membranes (Hofer et al., 2014). For induced lipid peroxidation, the increase in green fluorescence was linear the first h after addition of cumOOH and data were fitted using linear regression with calculation of slopes using CLARIOstar® MARS 3.00 software. For background lipid peroxidation (no inducer added; the rate of lipid peroxidation was orders of magnitude lower compared to when having added the inducer), data between 0 and 5 h were fitted also using linear regression.

2.8. Gene expression analysis

2.8.1. Dose selections and exposures for gene expression experiments in rat CGNs

In order to gain further insight into the observed mixture-induced effects, we evaluated the transcriptional responses of a panel of 60 genes in rat CGNs by qPCR assay. These genes were selected based on their role in the DNA damage response and repair pathway, apoptosis, Alzheimer's disease, Parkinson disease, oxidative stress signalling, oestrogen signalling, NMDA-R signalling, BDNF signalling, insulin signalling, and MAPK signalling pathways. For the assessment of genes affected by 24 h exposure to the seven mixtures, rat CGNs were at DIV 8 exposed in triplicate wells to two different concentrations of the 7 mixtures (n = 6 independent experiments, each from a separate cell isolation). One marginally cytotoxic concentration and one sub-toxic concentration were selected. 0.1% DMSO was included as a negative control. For selection of concentrations, further range finding studies were undertaken in addition to the concentration–response experiments, with a 1:3 dilution (333x human blood values) and a 1:3.5 dilution of the mixture stocks (286x human blood values). No cytotoxicity was detected with the MTT assay at these concentrations (n = 3) for any of the mixtures (data not shown). For exposure in the gene studies a 333x concentration was thus chosen as the sub-toxic concentration, whereas a 500x concentration was chosen as the marginally cytotoxic concentration, due to a small reduction in cell viability at this concentration for several of the mixtures in the concentration–response studies.

2.8.2. RNA isolation

Total RNA was isolated from the 333x or 500x blood concentration level exposed CGNs using the Quick-RNA™ MiniPrep Plus according to the manufacturer's protocol. RNAs were isolated from six independent experiments. RNA quantity and integrity purity were assessed as previously described (Duale et al., 2014a; Aarem et al., 2016) using a NanoDrop 1000 Spectrophotometer (Thermo Scientific, Norway) and Agilent 2100 Bioanalyzer according to the manufacturer's instructions (Agilent Technologies, Norway). RNA purity was estimated from the OD 260/280 and the OD 260/230 ratios. RNA integrity numbers (RIN) from 1 to 10 (low to high RNA quality) were calculated using the 2100 Expert software (Agilent Technologies, Norway). All samples were stored at −80 °C prior to gene expression analysis.

2.8.3. Quantitative real time PCR (qPCR) assay

The reverse transcription reaction and real-time qPCR were carried out as previously described (Duale et al., 2010, 2014b). In brief, total RNA (0.5 μg) from each sample was reverse transcribed to cDNA using the High Capacity cDNA Reverse Transcription Kit according to the manufacturer's protocol. The resulting reverse transcription reaction product was stored at −20 °C for further analysis.

Gene specific qPCR was carried out in 384 well PCR plates as previously described (Gutzkow et al., 2016) using KAPA SYBR® FAST qPCR Master Mix (2X) Universal Kit according to the manufacturer's protocol on a CFX384 Touch™ Real-Time PCR Detection System (Bio-Rad, Norway). In brief, a 1:40 dilution of cDNA from each sample was run for each gene of interest. All samples were analysed on the same 384-plate (96 samples; 8 treatment groups × 2 different concentrations × 6 independent experiments). This qPCR layout allowed simultaneous measurement of all samples in one 384-well plate, reducing errors due to run-to-run variations. A melting curve analysis, non-template controls (NTC) and non-reverse transcriptase controls (NRT) were included in each run. The gene specific primers were designed as previously reported (Brevik et al., 2012; Duale et al., 2014b) using the online Universal Probe Library System (Roche Applied Systems, Oslo, Norway).

2.8.4. Data pre-processing

The quantification cycle (*Cq*) values were recorded with CFX Manager™ Software (Bio-Rad, Norway). The raw *Cq* values were analysed by the comparative *Cq* – method (Livak and Schmittgen, 2001; Schmittgen and Livak, 2008) as previously described (Duale et al. 2010, Duale et al., 2012). In brief, prior to normalisation, the raw data *Cq* values were pre-processed and outliers were excluded from further analysis. In addition, target genes with Cq-values > 35 were considered beyond the limit of detection (LOD) and all Cq-values > 35 were replaced by Cq (LOD) + 1 (i.e. 35 + 1: Cq = 36). Filtering criteria for missing values was set to 70%, which is the minimum percentage of existing values, and all the patterns with<70% existing values were removed. The raw *Cq* values were then normalised using the geometric mean of four stably expressed reference genes, [this is given by ΔCq; where ΔCq (sample) = *Cq* (target gene) – *Cq* (average of reference genes)], and the ΔCq values were transformed to linear scale [normalised relative quantities (NRQ) = $2^{-\Delta Cq}$]. The fold change between treated and control samples were then calculated by dividing the NRQ values of the treated samples by the average NRQ value of the control samples (calibrators; reference sample). The fold change values were then log2-transformed in order to make the values symmetrical around zero. The stability of five reference genes was evaluated by the NormFinder algorithm (Andersen et al., 2004) and by their CV (%)-score. The stability score was calculated based on the NormFinder stability value and CV (%)-score. The geometric mean of the four most stably expressed reference genes (*Tbp, Hsp1b, Gusb* and *Actb*) were used for normalisation. The results of reference gene stability evaluation are presented in Supplementary Figure S2.

2.9. Western blot analysis

2.9.1. CD-1 mice cerebella

Frozen tissue of entire cerebella was kept on ice and homogenised in TE-buffer (10 mM Tris, 1 mM EDTA, pH = 8) with protease inhibitors leupeptin (5 μg/μL), pepstatin A (1 μg/μL), PMSF (300 μM), and phosphatase inhibitor Na_3VO_4 (100 μM) with a motorised pellet pestle (Sigma-Aldrich, St. Louis, US) before addition of SDS (2%) and further homogenisation through a 22G needle. An appropriate volume of buffer was 0.1 ml/10 mg of cerebellar tissue. Pierce® BCA Protein Assay Kit was used to determine total protein concentration before proteins were analysed with a standard western blot protocol (Sørvik and Paulsen, 2017) using primary antibodies against PAX6 (1:10000) GluN2B (1:1000) or β-ACTIN (1:5000), and then with HRP conjugated secondary antibody (1:10000, donkey anti-rabbit for GluN2B and goat anti-mouse for β-ACTIN). Immunoreactive proteins were detected using a chemiluminescence gel documentation system (Syngene, Cambridge, UK) with Luminata HRP detection substrates (Luminata Western Classico for PAX6 and β-ACTIN and Luminata Western Crescendo for GluN2B). Images were analysed in ImageJ. Initially a time study of PAX6 and GluN2B levels in control mice was conducted from 3 animals, sacrificed at each of the following time points: 7 days and 3, 6 and 9 weeks. Due to the dynamic expression of protein levels at 3 weeks of age, further studies of PAX6 and GluN2B levels were conducted at this time-point in control, Low POPs and High POPs animals. In total, protein levels from 9 different animals, were analysed in each of the three groups. Three gels were run, with samples from 3 animals from each group on each gel. On each gel PAX6/GluN2B protein levels were expressed as a ratio of levels in the internal standard β-ACTIN to adjust for differences in protein amount and blotting efficiency. The resulting levels were thereafter normalised and expressed relative to the average of the controls on the

respective gels set to a value of 1 for the exposure studies. For the time studies in the control mice, levels of PAX6/GluN2B were expressed relative to the average of protein levels measured at day 7, set to 1.

2.9.2. Chicken cerebella

To assess effects of PFOS exposure on GluN2B protein expression in the developing chicken cerebellum, eggs were either not injected (untreated) or injected with 50 μl per 50 g egg (50 ml fluid) of 1 mM PFOS (corresponding to a concentration of 27 μg PFOS per egg) or 1% DMSO in 0.9% NaCl at ED14 (n = 3 eggs per group), resulting in an approximate exposure concentration in the egg of 1 μM PFOS or 0.01‰ DMSO. Protein levels were assessed by western blotting and immunochemistry in cerebella isolated at ED17. Preparation of samples and western blotting were performed as described above.

2.10. Statistical analysis

Statistical analysis were conducted using PRISM 7 or SPSS v24 software. Normal distribution and equality of variances was tested for all data or was otherwise assumed e.g. in the cases of small sample sizes. Effects on cell viability after exposure of rat CGNs to the seven mixtures and chicken CGNs to PFOS as well as ROS production, lipid peroxidation, gene expression and PAX6/GluN2B expression in mice cerebella were assessed with one-way ANOVA and Dunnett's post hoc tests. For the gene expression data a Tukey's HSD post hoc test was applied to allow for multiple comparisons, i.e., comparison of the treatment groups (ΔCq of treated sample versus ΔCq of vehicle treated control). Best fit concentration–response curves for cell-viability and estimation and comparison of EC_{50} values after exposure to the four PFAA containing mixtures (PFAA, Cl + PFAA, Br + PFAA and Total mixture) were obtained by non-linear regression using a 4-parameter variable slope model, after log transformation of concentrations. Effects of CPP treatment on mixture-induced changes in cell viability, and GluN2B protein expression in chicken cerebellum were assessed with two-tailed paired Student's t-tests. For the lipid peroxidation rates, data (slopes of the curves) obtained by linear-regression were transformed into daily %-values of the respective DMSO controls (with or without cumOOH) set to 100%, allowing pooling of normalised data from different days. Unless otherwise stated, data were expressed as means ± standard error (SEM). In all the experiments conducted, a p-value of < 0.05 was regarded as statistically significant. For gene expression data the p-value was adjusted using Benjamini-Hochberg (BH) correction method.

For multivariate analysis, the gene expression dataset was log-transformed and UV-scaled in SIMCA-P (version 15; Umetrics AB, Umeå, Sweden). Principal component analysis (PCA) was used for an initial multivariate data analysis with the primary purpose of detecting potential outliers and identify clustering patterns. For the detection of clustering and extraction of the most discriminant variables, an orthogonal partial least-squares-discriminant analysis (OPLS-DA) was done. In these discriminant analyses, a default seven-round cross-validation was applied. The cross-validation analysis of variance (CV-ANOVA) was calculated to assess the reliability of the models. A summary of the resulting models is included in Supplementary Table S3. For the selection of the most discriminant genes, we considered the variable importance in the projection values (VIPp value) corresponding to the predictive component and set up a cut-off VIPp value ≥ 1 and a p(corr) (a vector representing the correlation, hence the reliability, to Y) $\geq \pm 0.5$.

3. Results

3.1. Mixture-induced effects on cell viability

3.1.1. Cell viability in rat CGNs after 24 h mixture exposure at DIV 8

CGNs were exposed to 250, 500, 1000, 2000, 3000 and 4000x human blood levels of the 7 mixtures for 24 h and viability assessed with the MTT-assay (Fig. 1). For the single mixtures both the PFAA mixture and the Cl mixture significantly decreased viability at concentrations from 1000x human blood levels and above (ANOVA ($F_{6,21} = 32.58$, $p < 0.001$) and ($F_{6,21} = 121.6$, $p < 0.001$)) where 53 and 12 percentage points reductions were observed ($p < 0.001$ and 0.05, respectively). For the Br mixture no significant effects on viability were observed at any of the tested concentrations. For the combined Cl + PFAA mixture, the Br + PFAA mixture as well as the Total mixture, viability was significantly decreased from a concentration of 500x human blood levels (ANOVA ($F_{6,21} = 157.8$, $p < 0.001$), ($F_{6,21} = 84.1$, $p < 0.001$) and ($F_{6,21} = 110.2$, $p < 0.001$)) where 16, 27 and 24 percentage point reductions were detected ($p < 0.05$ for the first and $p < 0.01$ for the two last, respectively). For the combined Cl + Br mixture effects on viability were significant from exposures of 3000x human blood levels (ANOVA ($F_{6,21} = 8.37$, $p < 0.001$)) where a reduction of 23 percentage points was observed ($p < 0.05$).

For the four mixtures containing PFAAs, concentration response curves were constructed and LC_{50} values computed (Supplementary Figure S4). The LC_{50} values were found to be significantly different when the curves for the PFAA mixture (LC_{50}: 953x human blood levels (95% CI [861,1056]), Hill-slope: −4.0), Cl + PFAA mixture (LC_{50}: 786x human blood levels (95% CI [704,878]), Hill-slope: −4.1), Br + PFAA mixture (LC_{50}: 756x human blood levels (95% CI [654,875]), Hill-slope: −3.2) and Total mixture (LC_{50}: 776x human blood levels (95% CI [694,868]), Hill-slope: −3.0) were compared (4-parameter model with top and bottom values constrained to 0 and 100%, respectively, $p = 0.02$).

3.1.2. Cell viability in rat CGNs measured at DIV 8, after mixture exposure at DIV 0

To assess effects of mixture exposure in undifferentiated cells, CGNs were also exposed for 8 days from DIV 0 to DIV 8 with 500 and 1000x of the seven mixtures, before measurements of cell viability were conducted. No effects on viability were detected when cells were exposed at this stage with any of the mixtures, and cells developed their normal interconnecting network of neurites, as assessed by light microscopy (results not shown).

3.2. Mechanistic studies on NMDA-R involvement in mixture-induced cell death in rat CGNs

When CGNs were co-incubated with 1000x of the PFAA and Total mixtures in conjunction with 10 μM CPP, cell viability was significantly improved as compared to treatment with the mixtures alone. Viability was increased from a mean value of 60 to 100 and from 38 to 99% of the DMSO control, respectively ($p < 0.05$ for both). On the other hand, when cells where co-treated with CPP and 3000x of the Cl mixture, viability was significantly reduced from 86 to 64% of the DMSO control compared to treatment with the mixture alone ($p < 0.05$) (Fig. 2).

3.3. Mixture-induced ROS production and lipid peroxidation in rat CGNs

3.3.1. ROS production after acute and 24 h exposure

Acute (1000, 2000 and 4000x human blood values) or 24 h (500, 1000 and 2000x human blood values) exposure to the seven mixtures had no significant effect on intracellular CGN ROS production as measured with the DCF assay (Supplementary Figure 5A and B).

3.3.2. Lipid peroxidation after mixture exposure

For the experiments conducted without inducer, no increase in the rate of lipid peroxidation was observed, however a significant decrease in lipid peroxidation rate was observed for three of the mixtures (ANOVA ($F_{14,129} = 4.65$, $p < 0.001$)): 27% ($p < 0.05$) for the PFAA and 28% ($p < 0.01$) for the Br + PFAA mixtures at 1000x human blood levels, and 24% ($p < 0.05$) for the Cl + PFAA mixture at 500x human blood levels (Fig. 3A). For experiments conducted with the inducer cumOOH, a

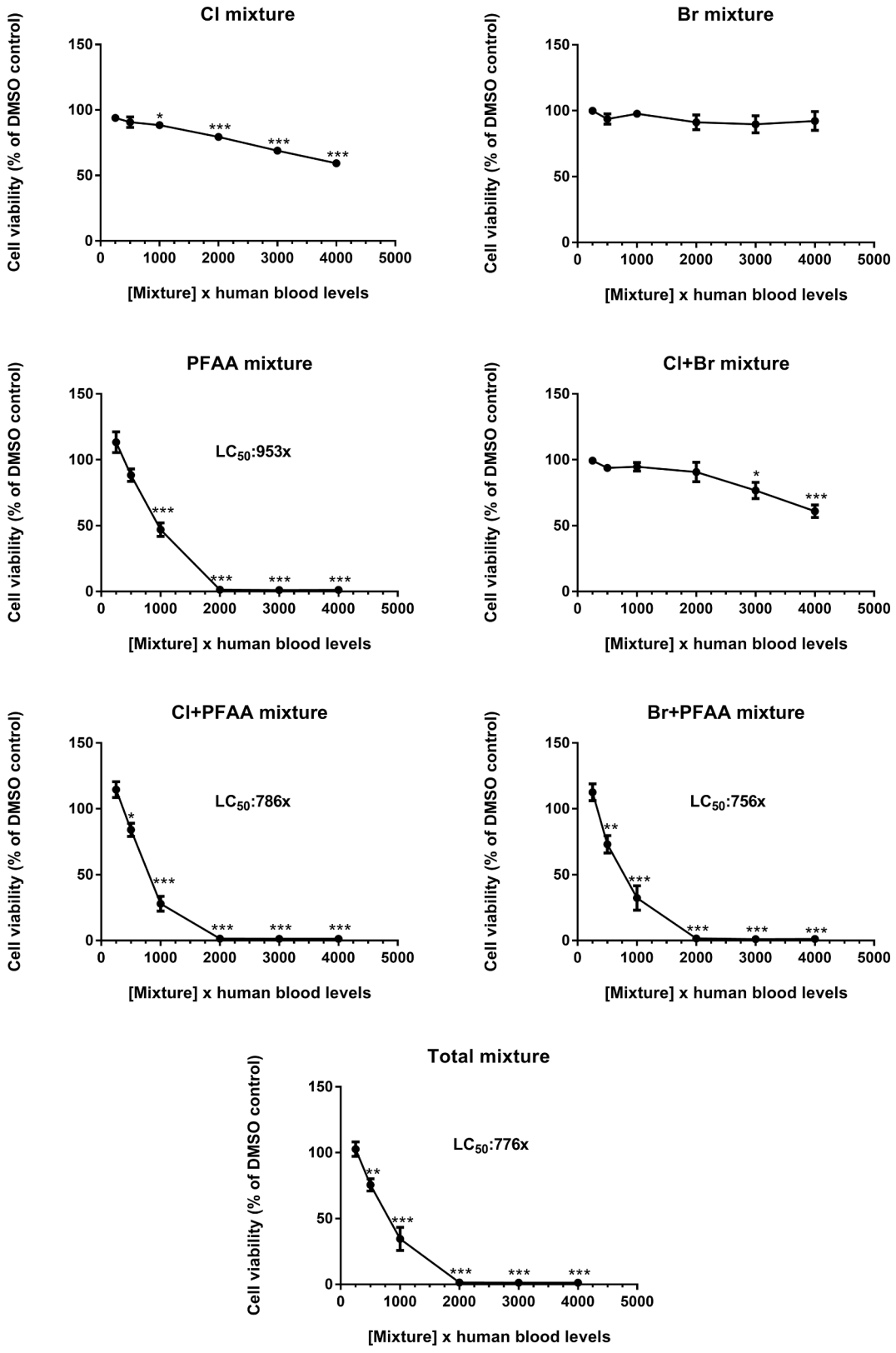

Fig. 1. Concentration dependent effects of a human blood-based mixture and sub-mixtures of persistent organic pollutants (POPs) on cell viability in rat cerebellar granule neurons. Cells were exposed at days *in vitro 8* for 24 h to increasing concentrations of the mixtures. Viability was assessed with the MTT assay (n = 4 independent experiments, each from a separate cell isolation, with each condition tested in triplicate) and expressed as % of the DMSO control set to 100%. Statistical differences from the DMSO control are indicated with *, ** and *** for $p < 0.05$, 0.01 and 0.001, respectively. LC_{50} values for the PFAA-containing mixtures are displayed. Abbreviations: LC_{50} = lethal concentration 50, [Mixture] = Mixture concentration, x = times.

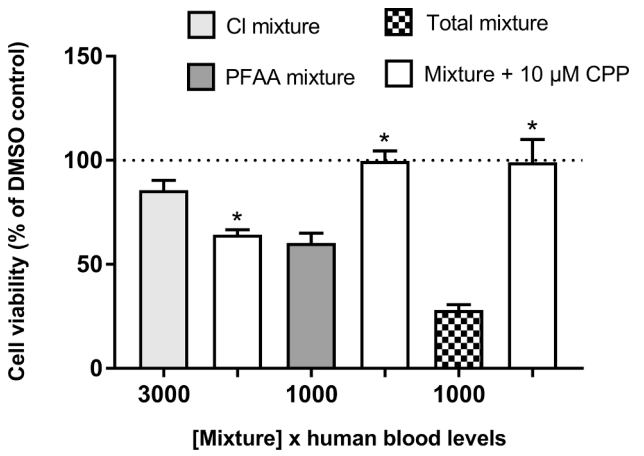

Fig. 2. Effects of CPP on POP mixture-induced toxicity in rat cerebellar granule neurons. Cells were exposed for 24 h to the Cl mixture (3000x human blood levels) as well as the PFAA and Total mixtures (1000x human blood levels), alone or in conjunction with the competitive N-methyl-D-aspartate receptor (NMDA-R) antagonist CPP (n = 3 independent experiments, each from a separate cell isolation, with each condition tested in triplicate). Cell viability was assessed with the MTT assay, and expressed as % of the DMSO control set to 100%. Statistically significant effects between cells exposed with and without CPP are indicated with * for $p < 0.05$. Abbreviations: POPs = Persistent organic pollutants, [Mixture] = Mixture concentration, x = times.

significant increase in the rate of lipid peroxidation was detected after exposure to the 7 mixtures (ANOVA ($F_{16,206} = 30.56, p < 0.001$)). At the 500x human blood levels concentration only the Total mixture significantly increased lipid peroxidation with 49% ($p < 0.001$), whereas at 1000x human blood levels all the four PFAA containing mixtures caused significant increases, specifically 36% for the PFAA and Br + PFAA mixtures ($p < 0.05$), 32% for the Cl + PFAA mixture ($p < 0.05$) and 43% for the Total mixture ($p < 0.01$) (Fig. 3B).

When CGNs were exposed at DIV 8 in 96 well plates to 1000x of the Cl mixture, the PFAA mixture, the Cl + Br mixture, the Cl + PFAA mixture, the Br + PFAA mixture or the Total mixture for 5 h, under the same conditions as used for the lipid peroxidation assay, no significant effects on viability were observed. This would indicate that the measured lipid peroxidation was occurring in presumably healthy cells (results not shown).

3.4. Gene expression studies in rat CGNs after 24 h mixture exposure at DIV 8

As described in 2.8.1 we evaluated the transcriptional responses of a panel of 60 genes in rat CGNs by qPCR assay. All treated samples were compared to the vehicle treated control samples (0.1% DMSO). Only those genes that passed the quality assurance criteria described in 2.8.4 were used. Following a quality assurance, removing genes with an inadequate measurement, we ended up with a matrix of 53 genes × 96 samples (96 samples; 8 treatment groups × 2 different concentrations × 6 independent experiments), and this matrix was used for downstream analysis. The normalised data of the 53 genes were used to calculate fold difference between treated and control samples.

We then conducted hierarchical clustering analysis (average-linkage and Euclidean distance similarity measurement) in order to group samples from different treatment-groups based on their transcript level similarity using the MeV software v4.7 (Saeed et al., 2006). The hierarchical clustering analyses results were visualised in a dendrogram and are presented in Supplementary Figure S6. By visual inspection of the clustering dendrogram, we observed that treatment with the seven mixtures did not give a definite clustering pattern, and biological replicates from the same treatment did not always cluster close to each

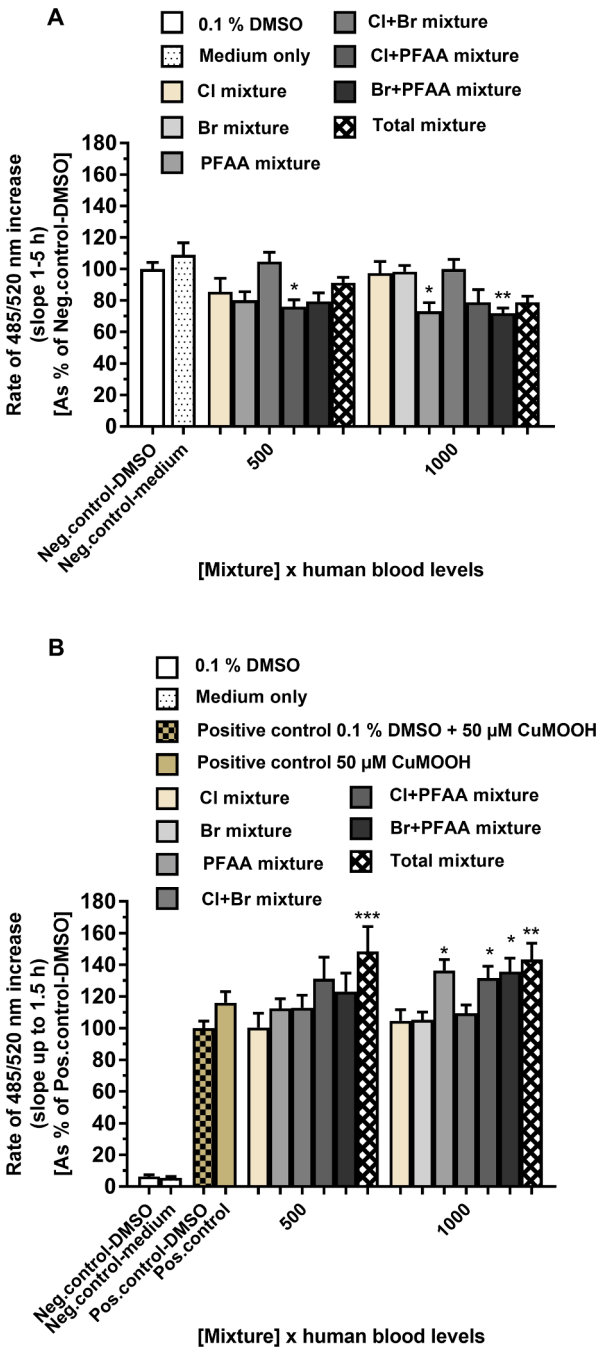

Fig. 3. Effects of human blood-based mixtures of persistent organic pollutants (POPs) on lipid peroxidation in rat cerebellar granule neurons. A) Lipid peroxidation was assessed during 5 h using the probe C_{11}-BODIPY after treatment of cells with increasing concentrations of a Total mixture or sub-mixtures of POPs. The slopes for the increase in green fluorescence (reflecting rate of lipid peroxidation) for each exposure were determined by linear regression and expressed as % of the slope for the 0.1% DMSO control. Mean values + SEM are displayed. B) Lipid peroxidation was assessed during 1.5 h using the probe C_{11}-BODIPY, after co-treatment of cells with 50 μM cumOOH and increasing concentrations of the same mixtures as used in A). The slopes are expressed as % of the slope for 0.1% DMSO + 50 μM cumOOH. Mean values + SEM are displayed. For both A and B, n = 3 independent experiments, each from a separate cell isolation, with each condition tested in triplicate. *, ** and *** indicate statistically significant differences ($p < 0.05$, $p < 0.01$ and $p < 0.001$) relative to the respective controls (0.1% DMSO in A, and 0.1% DMSO + cumOOH for B). (For interpretation of the references to colour in this figure legend, the reader is referred to the web version of this article.)

other. However, samples from cells treated with 500x human blood levels seemed to cluster close to each other and shared a similar expression pattern. A similar clustering pattern was also observed from the 333x human blood levels treated samples.

The relative transcript levels of the 53 genes are shown in Supplementary Table S7 and S8 for cells treated with mixtures at 333x and 500x blood levels, respectively, and a gene was characterised as statistically significantly differentially expressed when $p < 0.05$ with a fold change over ± 1.5. In the 333x human blood levels exposed group, five genes (*Prdx6*, *Sirpa*, *Esr2, Hmox1* and *Nr4a1*) were significantly upregulated, while eight genes (*Dcx, Stxbp1, Syp, Apex1, Mapk14, Gstp1, Grm4* and *Snap25*) were significantly downregulated following treatment with one or several of the mixtures compared to controls (Supplementary Table S7). In the 500x human blood levels exposed group, 31 genes were statistically significantly differentially expressed following treatment with one or several of the mixtures compared to controls; fifteen genes were upregulated, while sixteen genes were downregulated (Supplementary Table S8). Treatment of CGNs with the 500x mixtures significantly affected more genes than treatment with the 333x mixtures (Supplementary Tables S7 and S8). In all treatment groups, the transcript levels of two genes, *Prdx6* and *Sirpa* were statistically significantly upregulated following the treatment compared to the control group (Supplementary Tables S7 and S8). Furthermore, the transcript level of the four genes *Hmox1*, *Sod3*, *Srxn1* and *Esr2* were significantly upregulated, while *Stxbp1* was significantly downregulated following 500x human blood levels of PFAA mixture, Br + PFAA mixture, Cl + PFAA mixture and Total mixture treatments (Supplementary Table S8). *Casp4* gene was also upregulated upon PFAA mixture, Br + PFAA mixture, Cl + PFAA mixture and total-mixture treatments, however, the observed upregulation following Br + PFAA mixture treatment did not reach statistical significance (Supplementary Table S8). Among the sixteen downregulated genes in the 500x treatment groups, ten genes (*Mapk14, Hip1, Mapk8ip2, Syp, Pax6, Map3k10, Snap25, Madd, Grin2b* and *Stxbp1*) were significantly downregulated following 500x human blood levels of Br + PFAA mixture and Cl + PFAA mixture (Supplementary Table S8), and some of these genes were also downregulated following PFAA or Total mixture treatments (Supplementary Table S8).

The use of a multivariate analysis facilitates the interpretation of the results as it aims to identify systematic patterns across the samples. We created significant OPLS-DA models for the 333x total and the Cl + PFAA mixtures vs the control. Whereas all the mixtures but the Cl were significant at 500x concentrations when compared with the control (all CV-ANOVA, $p < 0.05$) (See Table S3). At 333x, the Total and Cl + PFAA mixtures shared 5 genes, namely *Prdx6, Camk2, Esr2, Map3k10 and Aifm1*. Interestingly, the downregulation of *Syp* and *FOXO3* was relevant in the Cl + PFAA but not in the Total mixture. The treatment with mixtures containing PFAAs at 500x concentration seems to have effect on more genes. Whereas mixtures without PFAAs show less unique genes modulated. A detailed list of the relevant features on each significant model is shown in Table 2.

IPA core analysis (QIAGEN, Ingenuity Pathway Analysis) was performed to gain more insight into the underlying molecular mechanisms of the 500x mixture exposure on the expression pattern of the 53 genes, and the top significantly ($p < 0.01$) enriched pathways and their associated genes are presented in Table 3. Genes involved in canonical pathway categories (cardiac necrosis/cell death, liver necrosis/cell death, long-term renal injury anti-oxidative response Panel, NRF2-mediated oxidative stress response or xenobiotic metabolism signalling) were enriched in cells treated with PFAA, Br + PFAA, Cl + PFAA or Total 500x mixtures (Table 3). Only few canonical pathway categories were enriched in cells treated with Br, Cl or Cl + Br mixtures (Table 3).

Table 2
Most discriminantly expressed genes of cerebellar granule neurons treated with mixtures of POPs at 333x and 500x serum levels compared to DMSO controls according to significant OPLS-DA models.

Mixture	Genes
Total mixture, 333x	Prdx6, Sirpa, Camk2, Hmox1, Esr2, Map3k10, Mapk14, Adrb2, Gpx4, Gstk1, Aifm1, Dscr1l2
Cl + PFAA mixture, 333x	Stxbp1, Grin2a, Camk2, Syp, Foxo3, Dcx, Map3k10, Prdx6, Esr2, Hmox2, Mapk8ip2, Aifm1
Total mixture, 500x	Prdx6, Hmox1, Sirpa, Srxn1, Casp4, Hip1, Nfe2l2, Sod3, Stxbp1, Gstk1, Gper1, Map3k10
PFAA mixture, 500x	Prdx6, Hmox1, Srxn1, Sod3, Sirpa, Dhcr24, Nfe2l2, Casp4, Esr2, Gstk1, Hip1, Snap25, Casp9,
Br + PFAA mixture, 500x	Prdx6, Sirpa, Stxbp1, Foxo3, Snap25, Hmox1, Hmox2, Madd, Casp3, Hip, Casp4, Esr2, Grm4, Dhcr24
Cl + PFAA mixture, 500x	Prdx6, Sirpa, Srxn1, Madd, Hmox1, Sod3, Hip1, Dhcr24, Hmox2, Camk2
Cl + Br mixture, 500x	Prdx6, Sirpa, Hip1, Foxo3, Mapk1, Foxo1
Br mixture, 500x	Prdx6, Sirpa, Apex1, Sod3, Esr2, Syp, Grin2b

The Total mixture contained 29 different POPs from three groups consisting of 16 chlorinated (Cl), 7 brominated (Br) and 6 (PFAA) perfluorinated compounds. The Cl + PFAA mixture contained 16 Cl and 6 PFAA compounds, the Br + PFAA mixture 7 Br and 6 PFAA compounds, and the PFAA mixture 6 PFAA compounds. The concentrations of the different POPs were kept constant between the mixtures. The genes selection was based on a cutoff value of VIP < 1 and a p(corr) < 0.05.

3.5. Protein expression analysis

3.5.1. Protein expression analysis of cerebellum from in vivo mixture-exposed mice

A time study of control mice showed that PAX6 levels were significantly lower at 3, 6 and 9 weeks as compared to day 7 (ANOVA ($F_{3,8} = 8.45$, $p < 0.01$)), $p < 0.01$ for all (Fig. 4A). Furthermore, levels of GluN2B were higher on day 7 and week 3 than in week 6 and 9, and when compared to week 3, values at week 6 and 9 were significantly lower (ANOVA ($F_{3,11} = 6.07$, $p < 0.05$)), $p < 0.05$, for both (Fig. 4B). A representative Western blot for the time study is shown in Fig. 4C. During analysis of samples from animals sacrificed at three weeks of age we found that offspring from mothers fed the high POP diet had significantly lower levels of PAX6 (ANOVA ($F_{2,23} = 10.11$, $p < 0.001$)), whereas offspring from mothers fed the low POP diet had significantly lower levels of GluN2B (ANOVA ($F_{2,23} = 12.23$, $p < 0.001$)) than offspring from control mothers, $p < 0.01$ for both (Fig. 4D and E). Results were excluded from one animal for PAX6 from the High POPs group and from one animal for Glu2NB from the Low POPs group, due to being identified as significant outliers using Grubbs' test ($p < 0.01$). Representative Western blots for the exposure studies are shown in Fig. 4F.

3.5.2. Effects on GluN2B protein expression in chicken cerebellum after inovo exposure to PFOS

To assess effects of PFOS on the developing cerebellum, eggs were injected with PFOS to a concentration of 1 μM in the egg at ED 14. Western blot analysis of PFOS treated cerebella isolated at ED 17 showed a statistically significant reduction in GluN2B protein-levels as compared to the DMSO treated controls ($p < 0.05$) (Supplementary Figure S9).

To verify toxicity in isolated chicken CGNs within the same concentration interval as previously observed in rat CGNs, exposure to 10 and 100 μM PFOS was conducted for 24 h, at DIV 2, in CGNs from chicken isolated at ED 17. Viability was significantly affected at 100 μM (ANOVA ($F_{2,6} = 18.69$, $p < 0.01$)) with a reduction of 92 percentage points as compared to the 0.2% DMSO control ($p < 0.01$) (Supplementary Figure S10).

Table 3
Top enriched IPA canonical pathways.

Ingenuity Canonical Pathways	500X-mixture (-log(p-value))							Genes
	PFAA	Br	Br+PFAA	Cl	Cl+PFAA	Cl+Br	Total	
Cardiac Hypertrophy	2.90		2.96	2.55	2.06	2.23	2.54	ESR2,FOXO3,MAPK1,MAPK14
Aryl Hydrocarbon Receptor Signaling	5.78		3.05		1.87	2.99	7.01	ESR2,GSTK1,GSTP1,MAPK14,NFE2L2
Oxidative Stress	3.32	6.53	8.19		8.37		9.30	GPX1,MAPK14,NFE2L2,PRDX6,SOD1,SOD2,SOD3
Renal Necrosis/Cell Death	2.41		5.41		8.21	1.90	6.98	CASP3,CASP4,GRIN2B,HIP1,HMOX1,MAPK14,PARK7,SOD1,SOD2
Cardiac Necrosis/Cell Death	3.20		8.76		7.54		4.18	CASP3,FOXO1,FOXO3,HMOX1,HMOX2,MAPK1,MAPK14,NFE2L2,PARK7,SOD2
Liver Necrosis/Cell Death	1.85		4.46		7.38		2.78	CASP3,FOXO3,HMOX1,MAPK14,MAPK9,NFE2L2,SOD1,SOD2
Long-term Renal Injury Anti-oxidative Response Panel	4.34		5.92		8.46		4.10	HMOX1,SOD1,SOD2,SOD3
NRF2-mediated Oxidative Stress Response	6.83		6.51		8.27		7.85	GSR,GSTK1,GSTP1,HMOX1,MAPK1,MAPK14,MAPK9,NFE2L2,SOD1,SOD2,SOD3
Xenobiotic Metabolism Signaling	6.02		4.30		7.14		8.49	CAMK2A,GSTK1,GSTP1,HMOX1,MAP3K10,MAPK1,MAPK14,MAPK9,NFE2L2SOD3
Cardiac Fibrosis			2.49		2.58		3.08	GPX1,HMOX1,MAPK14,SOD2
Liver Proliferation			1.45		2.60		1.83	MAPK1,MAPK14,MAPK9,NFE2L2
LPS/IL-1 Mediated Inhibition of RXR Function	3.45				1.50		3.08	GSTK1,GSTP1,MAPK9,SOD3
Decreases Transmembrane Potential of Mitochondria and Mitochondrial Membrane			3.30		4.90			CASP3,MAPK14,MAPK9,SOD2
Glutathione Depletion - Phase II Reactions	4.24						4.00	GSTK1,GSTP1
Increases Transmembrane Potential of Mitochondria and Mitochondrial Membrane			4.55		4.65			CASP3,SOD2,SRXN1
Mitochondrial Dysfunction			4.32		4.46			CASP3,GSR,MAPK9,PARK7,SOD2
Positive Acute Phase Response Proteins			5.23		3.31			HMOX1,HMOX2,SOD2
Pro-Apoptosis			2.94		3.01			CASP3,FOXO3
TGF-β Signaling			2.21		3.77			MAPK1,MAPK14,MAPK9

Note. Top enriched canonical pathways following 500x mixtures treatment. Canonical pathways with a $p < 0.01$ are labelled in red colour. The representative differentially expressed genes in the canonical pathway are listed to the right.

4. Discussion

The present study shows that exposure to mixtures of POPs, based on average blood levels from the Scandinavian population, affect cell viability in rat CGNs from concentrations 500x human levels, whereas gene expression was affected at the lowest tested concentration of 333x human levels. Further, genetic markers and mechanistic studies indicate the involvement of oxidative stress and the NMDA-R in the induced toxicity, the latter mainly for the mixtures containing perfluorinated compounds. Additionally, we observed changes in the expression of two genes important for cerebellar development; *Pax6* and *Grin2b*. These changes were mirrored by differences in protein expression in the cerebellum of mice exposed *in utero* and throughout lactation to mixtures containing the same compounds, via their mothers. Although the concentrations applied in the present study were higher than the concentration calculated for the average Norwegian population, blood values of the various compounds would vary with geographical regions. E.g. would certain populations consuming a diet with high contents of POPs, such as the Inuit people, as well as people living close to POP contaminated areas, and also occupationally exposed workers, potentially exhibit higher body burdens, and blood levels of POPs.

4.1. Mixture-induced effects on cell viability

Our results show reduced cell viability after 24 h exposure of CGNs to the POP mixtures (Fig. 1). This is in contrast to exposure of cells for 5 h conducted concomitant with the lipid peroxidation assay, where no effects on viability were observed. The absence of an effect after 5 h is most likely the result of shorter exposure time, but the possibility that this is related to the use of 96 well plates (as opposed to 24 well plates at 24 h), may not be ruled out. After 24 h exposure of CGNs the PFAA mixture alone induced somewhat lower toxicity than the other PFAA containing mixtures as indicated by the LC_{50} values, where the potencies can be ranged: Br + PFAA mixture > Total mixture > Cl + PFAA mixture > PFAA mixture. Interestingly, the fact that the PFAA mixture exerts a stronger effect than the Cl and Br mixtures, and that the PFAA mixture in combination with the Br and/or Cl mixtures exerts a stronger effect than the PFAA mixture alone, indicates a degree of additivity between the mixtures. Thus, although the single PFAA/Cl mixtures and the combined Cl + Br mixture only significantly affected cell viability at 1000x and 3000x human blood values, respectively, whereas the Br mixture induced no significant toxicity up to 4000x human blood levels, the LC_{50} values, and significant effects of the combined Cl + PFAA/Br + PFAA/Total mixtures at 500x human blood levels, indicate that the Cl and Br mixtures add to the toxicity of the PFAA mixture at lower concentrations. Additive effects on toxicity and other effects in CGNs between non-coplanar PCB congeners have indeed been observed by others (Kodavanti and Ward, 1998), although at concentrations higher than the ones used in the present study. Additive inhibitory effects on glutamate uptake in rat synaptosomes have also been observed after exposure to HBCD, the pentaBDE mixture DE-71, the commercial PCB mixture Arochlor 1254 and PCB 153 in combination with MeHg (Stavenes Andersen et al., 2009), whereas Mariussen and Fonnum (2001) observed a more efficient inhibition of glutamate uptake by Arochlor 1242 and 1254, than by single PCB congeners. The lack of significant effects after exposure of CGNs to 500x of the Br, Cl and Cl + Br mixtures is in line with the absence of statistically significant upregulation of the *Casp4* gene after treatment with these mixtures (Fig. 1, Supplementary Table S8). As shown in Table 1, the perfluorinated compounds are present at higher levels in the mixtures than the other mixture compounds, reflecting their prominent presence in human blood, which may be a plausible explanation for the greater toxicity observed for the PFAA-containing mixtures. Of the perfluorinated compounds included in the mixture, PFOS occurs at the highest level. The estimated LC_{50} values for PFOS in the PFAA, Cl + PFAA, Br + PFAA and Total mixture would correspond to 15.6, 12.9, 12.4 and 12.7 μM, respectively (see Table 1), which is somewhat lower than the previously published LC_{50} value of 38 μM for PFOS as a single compound in the same cell system obtained using the MTT assay (Berntsen et al., 2017b) and 60 and 62 μM using the TB assay (Reistad et al., 2013; Berntsen et al., 2017b). The lack of significant effects on cell viability after exposure to 500x of the Cl mixture, may seem surprising, however as can be seen in Table 1, the concentrations of the chlorinated compounds included in the mixtures at 500x human blood values range from 9 to 544 nM. Previous studies report cytotoxicity of several of the included PCB congeners, however at considerable higher concentrations. As an example (Tan et al., 2004) observed loss of cell membrane integrity after 20 min exposure to 10 μM PCB 28 and 52. Further, exposure of CGNs to Arochlor 1242 and 1254 as

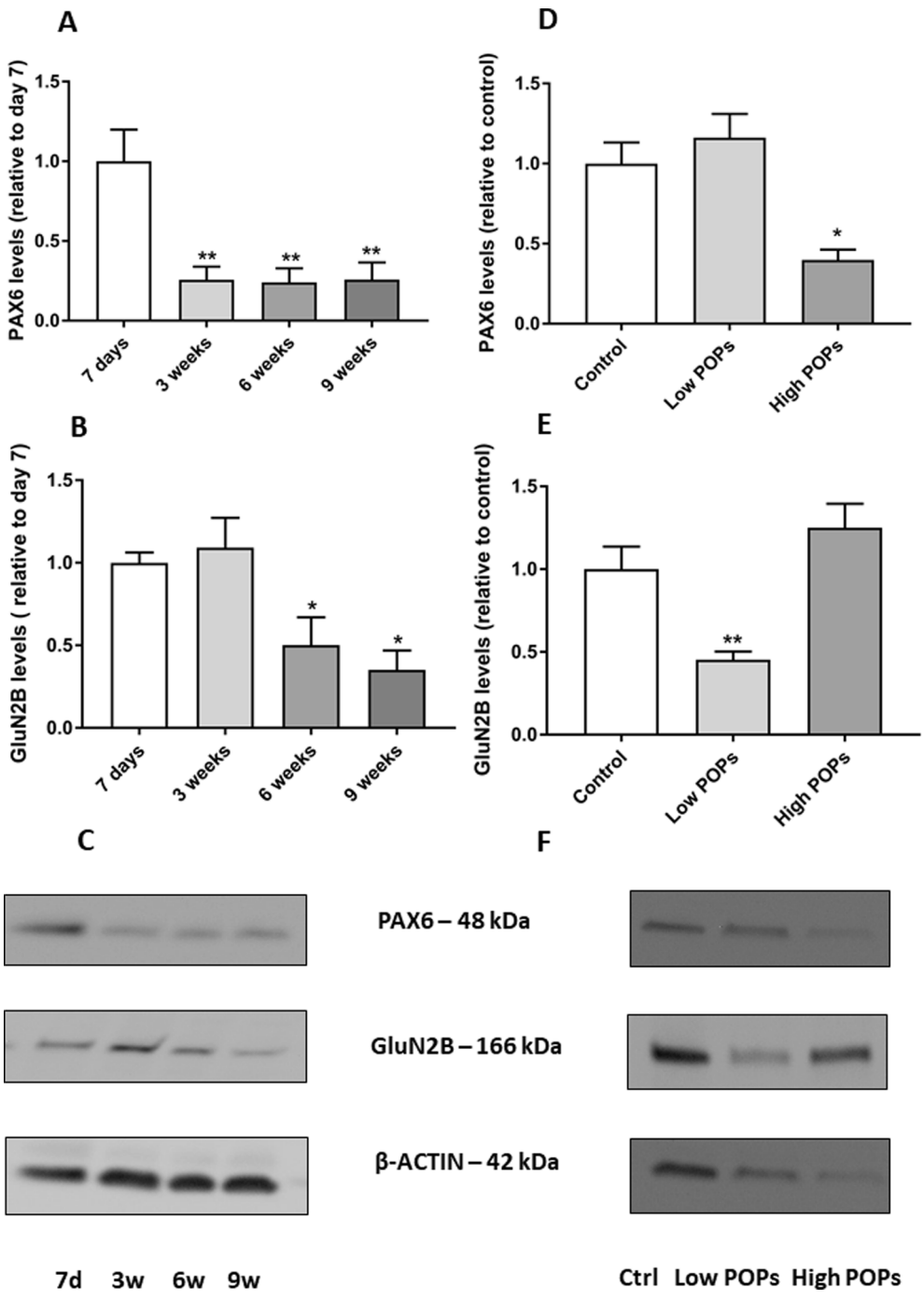

Fig. 4. PAX6 and GluN2B protein expression levels in cerebellum from maternally exposed CD-1 mice. A) and B) Time studies of mean PAX6 and GluN2B expression relative to day 7 in control animals from n = 3 animals at each time-point are shown, and C) a representative Western blot for PAX6, GluN2B and the internal standard β-ACTIN for control animals is shown. D) and E) show mean PAX6 and GluN2B expression levels, respectively, (n = 9 animals in each group) in 3 week old maternally exposed offspring from mothers exposed to feed with evaporated solvents (Control), from mothers exposed to feed containing a mixture of 29 different POPs including 16 chlorinated, 7 brominated and 6 perfluorinated compounds, giving a daily intake of POPs corresponding to 5000x hEDI, (Low POPs) or to mothers exposed to feed giving a daily intake corresponding to 100000x hEDI (High POPs). F) A representative Western blot for PAX6, GluN2B and the internal standard β-ACTIN from control and exposed animals is shown. *, ** and *** indicate statistically significant differences ($p < 0.05$, $p < 0.01$ and $p < 0.001$) relative to respective controls (protein levels at day 7 in A and week 3 in B and protein levels in control animals in D and E). Abbreviations: d = day, w = week, ctrl = control, POPs = persistent organic pollutants, hEDI = human estimated daily intake (this intake was adjusted to mice assuming a body weight of 25 g, and a feed intake of 3 g feed/day).

well as PCB 153, had significant effects on viability from concentrations of 25 μM for the first and 6.25 μM for the two latter, with LC_{50} values of 30, 10 and 8 μM, respectively (Mariussen et al., 2002). In studies with other compounds of the Cl mixture, *p,p*'-DDE significantly increased caspase-3-activity and LDH-release in mouse CGNs at concentrations from 10 μM and above after 6 and 24 h, but not at lower concentrations (Wnuk et al., 2016), whereas 30–300 μM lindane was reported to induce a concentration-dependent cytotoxic effect in mouse CGNs exposed for 24 h (Vale et al., 1998). Additionally, prolonged treatment of CGNs to 3 μM dieldrin, had no effect on viability as assessed by the MTT assay (Babot et al., 2007). As a result, although the Cl mixture only induced significant toxicity from a concentration of 1000x human blood levels, the concentrations of the individual components of the mixture at this dilution are considerably lower than concentrations of single chemicals previously reported to induce toxicity in cultures of CGNs. For the Br mixture, no significant toxicity in CGNs was induced even at a concentration of 4000x human values, however the relative concentrations of the brominated compounds in the mixture are even lower than concentrations of the chlorinated compounds; 1–33 nM at 500x and 5–262 nM at 4000x. In comparison, previous studies report effects on viability in CGNs after 24 h exposure to DE-71 and HBCD, with LC_{50} values of 3 and 7 μM, respectively (Reistad et al., 2006).

We have previously observed that PFOS induces rapid excitotoxicity in isolated CGNs from rats (Berntsen et al., 2018). Further, PFOS-induced, but not perfluoroalkyl carboxylic acid-induced toxicity was blocked by co-treatment with the NMDA-R antagonists MK-801, memantine and CPP. NMDA-R involvement has also been implicated in Arochlor 1254-induced effects on the viability of CGNs after use of MK-

801 (Mariussen et al., 2002). As described in AOP ID 48 (Spinu et al., 2019) excessive stimulation of the NMDA-R may lead to intracellular Ca^{2+} overload, mitochondrial dysfunction, cell injury or death, decreased synaptogenesis and neuronal network dysfunction followed by impairment of learning and memory in the child. Also, in the present study, we observed an almost complete reversal of cell viability effects induced by the total and PFAA mixtures with co-application of the competitive NMDA-R antagonist CPP, whereas for the Cl mixture cell viability was further decreased (Fig. 2). This makes it reasonable to assume that at least part of the effects on viability induced by the Total mixture may be attributed to the perfluorinated content of the mixture and based on our previous studies also to a large extent to PFOS. Interestingly, in a different study, concentrations of 20-200x blood levels of the Total *in vitro* mixture affected the behavioural endpoint - swimming speed - in zebrafish larvae. Here, this effect could be mimicked by exposure to the PFAA mixture, or by PFOS alone at a concentration of 100x blood levels (Khezri et al., 2017). The concentration of PFOS in the mixtures at 500x, the lowest tested concentration in the present study significantly affecting viability, is 8 μM. Such high concentrations are most likely only relevant in an occupational setting. There are no studies reporting levels of perfluorinated compounds in the brain from occupationally exposed workers, but levels of PFOS up to 180000 ng/ml (236 μM) have been reported in blood (Fu et al., 2016). Based on the human study by Maestri et al. (2006) and similar studies in wildlife (further discussed in Berntsen et al., 2017b) where approximately 25% of the levels in blood were detected in the brain, this would correspond to a concentration of 60 μM. It should be noted that cells in the present experiments were exposed to the mixtures in the absence of FBS and thus in the absence of serum proteins. As perfluorinated compounds in blood have a high affinity for plasma proteins, it could be expected that the toxicity of the perfluorinated containing mixtures in the presence of proteins would potentially be lower than presently observed. Although, a reduction in the toxicity induced by PCBs in CGNs has previously been reported after co-application of the non-competitive open channel blocker MK-801, in the present study we applied the competitive NMDA-R antagonist CPP, which may potentially contribute to absence of a protective effect of NMDA-R blockage after exposure to the Cl mixture. Additionally, the Cl mixture contains other chlorinated compounds apart from PCBs, which may have been the driving force in the toxicity at the tested concentration. Cerebellar granule cells are cultured in medium containing 25 mM KCl, inducing partially depolarising conditions, some stimulation of the NMDA-R and influx of Ca^{2+} necessary for the survival of the cells in culture (Gallo et al., 1987). As a result, the blocking of this receptor by CPP may have been enough to aggravate the toxicity already induced by the Cl mixture, which may explain the further reduction in viability.

The toxicity induced by the investigated mixtures seem to be dependent on the developmental stage of the cultures. When newly isolated immature CGNs from rat were exposed to the 7 mixtures from DIV 0 at plating to DIV 8, no toxicity was observed as compared to cells exposed at DIV 8. We have previously reported similar findings after exposure of cells at DIV 0 to PFOS (Berntsen et al., 2018). It is likely to assume that this lack of toxicity could be related to the immature status of the cells. When CGNs develop in culture, they differentiate morphologically, physiologically and biochemically (Gallo et al., 1982; Novelli and Henneberry, 1987; Thomas et al., 1989). For the first few days *in vitro*, CGNs have low responsiveness to glutamate (Schramm et al., 1990). With increasing time in culture, the CGNs develop the ability to release glutamate in a Ca^{2+}-dependent manner when exposed to a depolarising stimulus (Gallo et al., 1982), which occurs in parallel with the development of neurite, synaptic vesicle, and synapse formation (Thomas et al., 1989). In the rodent cerebellar cortex, as well as in neuronal cultures, major changes also occur in the expression of GluN2 subunits during development and maturation (Audinat et al., 1994; Vallano et al., 1996; Cebers et al., 2001), and changes in the NMDA-R subunit composition influences electrophysiological and signalling properties of the ion channel (Mori and Mishina, 1995; Yamakura and Shimoji, 1999). The GluN2B subunit, dominant during early development, is gradually replaced by GluN2A and GluN2C in mature post-migratory cells during the second post-natal week (Llansola et al., 2005). It has previously been shown that whereas the predominant GluN2 subunit expressed in cultures of rat CGNs from DIV 0 is *Grin2b* mRNA, at DIV 5 *Grin2a* predominates (Vallano et al., 1996). Also, at DIV 8 GluN2A proteins were found to be the predominant GluN2 NMDA-R subunit (Cebers et al., 2001).

4.2. *Mixture-induced effects on apoptotic pathways:*

A powerful approach to study cellular responses to environmental toxicants is to analyse alterations in gene expression patterns. The reduction in cell viability observed in the present study may be explained by several mechanisms of action. Caspases (casp) like CASP-4 may be involved in both inflammatory processes and apoptosis of nerve and glial cells (Suk et al., 2002; Fan et al., 2005; Scott and Saleh, 2007). Cleavage of CASP-4 is suggested to be activated by ER stress-inducing agents (Hitomi et al., 2004), and excessive or long-termed ER stress results in apoptotic cell death (Imaizumi et al., 2001). The expression level of the *Casp4* gene was significantly upregulated after treatment with 500x of three out of the four PFAA-containing mixtures, indicating an involvement of apoptotic pathways in mixture-induced cell death (Supplementary Table S8). The link between observed *Casp4* upregulation and apoptosis is further supported by differential expression of a number of genes involved in cell survival or death after exposure to several of the mixtures. The protein CASP-3, encoded by *Casp3* is in apoptotic cells, activated both by extrinsic (death ligand) and intrinsic (mitochondrial) pathways (Salvesen, 2002). Huntingtin-interacting protein 1 (*Hip1*) gene codes for an endocytic adaptor protein that contributes to fast synaptic transmission at excitatory synapses in the CNS (Metzler et al., 2007) and its overexpression is reported to induce neuronal cell death through CASP-3 activation (Choi et al., 2006). CASP8AP2 encoded by *Casp8ap2* has an important role in the apoptotic signalling complex to mediate Fas-induced apoptosis (Imai et al., 1999), whereas the *Foxo3* gene functions as a trigger for apoptosis through expression of genes necessary for cell death, such as the FasL gene (Brunet et al., 1999). MADD involvement is reported in blocking apoptosis of neuronal cells under conditions of cytotoxic stress (Miyoshi and Takai, 2004). *Map3k10* functions preferentially on the JNK signaling pathway and has been shown to be involved in nerve growth factor (NGF) induced neuronal apoptosis. Inhibitors of this kinase prevent activation of cell death processes and enhance cell survival signaling (Pedraza et al., 2009). *Mapk1* encodes a member of the extracellular signal-regulated kinases (ERKs) and is involved in a wide variety of cellular processes such as proliferation, differentiation, transcription regulation and development (Gerschutz et al., 2014). The observed decrease in expression levels of the above mentioned genes after exposure to 500x of one or several of the PFAA-containing mixtures may thus be an attempt to counteract apoptosis in the CGN culture. The DHCR24 protein encoded by *Dhcr24* encompasses enzymatic, antioxidant, and anti-apoptotic activities. DHCR24 is shown to exert a neuroprotective effect against ROS resulting from ER stress, and overexpression of *Dhcr24* was shown to inhibit apoptotic cell signaling (Lu et al., 2014), hence it seems reasonable to assume that the observed upregulation of *Dhcr24* is a counterbalance to prevent the commitment of the activated apoptotic pathway in CGNs. Activation of FOXO1 protein upregulate pro-apoptotic proteins including Fas ligand (FasL), or *trans*-activate BIM protein promoting apoptosis, thus upregulation of *Foxo1* gene expression level due to Total mixture exposure indicate activation of apoptotic signalling.

Brain mitochondria are essential for processes like neurotransmission, neuronal plasticity, cellular resilience to stress and also behavioural adaptation (Mattson, 2008). Interestingly, mitochondrial-regulated caspase activation is reported to be involved in modulation

of synaptic plasticity (Manoli et al., 2007). Overactivation of the NMDA receptor results in influx of Ca^{2+} into the cell, which is taken up by mitochondria and triggers the opening of the mitochondrial permeability transition pore. This reduces the mitochondrial membrane potential, reducing ATP production, which in turn may lead to insufficient glucose supply necessary for cell survival and processes such as long-term potentiation (LTP); a lasting increase in synaptic strength and signal transmission between neurons (Markham et al., 2014), mediated by influx of Ca^{2+} through the NMDA-R in the postsynaptic spine. At the cellular level, NMDA receptor-induced Ca^{2+} influx is almost exclusively cleared by the mitochondria (Wang and Thayer, 2002). Excessive Ca^{2+} influx into mitochondria may also release cytochorome c, starting the mitochondrial apoptotic cascade (Ow et al., 2008). The release of cytochorome c can be prevented by the transcription and release of pro-survival proteins like Bcl-2 (Kluck et al., 1997). This however, is dependent on the concentration of intracellular Ca^{2+} (Markham et al., 2014). The IPA analysis conducted for the genes expressed after exposure to 500x of the mixtures (Table 3) shows that decreased and even increased transmembrane potential of mitochondria and the mitochondrial membrane, in addition to mitochondrial dysfunction appear to be important pathways of toxicity after mixture exposure, at least for Cl + PFAA and Br + PFAA mixtures.

Overall, analysis of the most discriminantly expressed genes of the CGNs based on the OPLS-DA models, show that exposure to the highest POP concentration (500x serum levels) resulted in more differentially expressed genes related to apoptosis than the 333x serum level (Table 2). However, at 333x serum levels, the change in expression of apoptotic genes was not associated with significant effects on cell viability. This may partly be because some of the genes code for proteins with several possible roles in cell function in addition to apoptosis, as described above. Interestingly the gene *Aifm1* (apoptosis inducing factor mitochondria associated 1), showed up as one of the most discriminantly expressed genes for the Total and Cl + PFAA mixtures at 333x serum levels (Table 2), although it was not found to be significantly up- or downregulated in the univariate analysis (Supplementary Table S7). *Aifm1* is essential for nuclear disassembly in apoptotic cells. It is found in the mitochondrial intermembrane space, and its gene product is reported to be linked to the function of the apoptogenic proteins cytochrome *c* and caspase-9 (Cai et al., 1998). As may be visualised from Table 2, the Br or Cl mixtures alone did not induce changes to genes related to apoptotic pathways, in contrary to the PFAA and Cl + Br containing mixtures, the latter suggesting additive effects. The IPA analysis support that genes involved in pathways stimulating necrosis and cell death is enriched in the mixtures containing PFAAs, and in particular the Cl + PFAA mixture. Therefore, the PFAAs seems to dominate these responses, possibly partly due to their high content in human blood and thereby these mixtures, as discussed above.

4.3. Mixture-induced effects on redox signalling

No increase in ROS production was detected after exposure of CGNs to any of the mixtures using the DCF assay. Similarly, previous studies with acutely dissociated CGNs have not reported ROS production using the DCF assay after exposure to selected co-planar and non-coplanar PCBs (PCB 80 and 52) at concentrations up to 10 μM (Tan et al., 2004), which is higher than the maximum concentrations of PCBs used in our study (Table 1). Yet again ROS production was detected by Dreiem et al. (2009) after exposure of cells to 5–50 μM of various congeners of hydroxylated PCBs. Further, no ROS production was detected with this assay in CGNs exposed to μM concentrations of the brominated compound HBCD or the commercial pentaBDE mixture DE-71 (Reistad et al., 2006), whereas Blanco et al. (2011) did observe an increase in ROS after exposure to 25 μM BDE-99. Additionally, we have previously not found ROS production with the DCF assay for the six PFAAs included in the presently used mixture at concentrations up to 600 μM (Berntsen et al., 2017b), although ROS production after PFOS and PFOA exposure has been observed by others (Lee et al., 2012; Reistad et al., 2013). In the present study, the concentrations of the brominated compounds in the Total mixture at the highest tested concentration of 4000x human blood levels for the DCF assay would be in the nM range, whereas the chlorinated compounds would be at the low μM level. The most prominent perfluorinated compounds PFOA, PFHxS and PFOS would range from 26 to 65 μM (Table 1). The use of lower concentrations of single compounds in the present study than previously used by others, may partly be a possible explanation for the lack of ROS production observed here after use of the DCF assay, as may methodological differences. However, the discrepancies in ROS detection between different studies, and the lack of ROS production detected with the DCF assay despite several genetic markers indicating that oxidative stress is involved after exposure to the mixtures, suggest that this is perhaps not the most sensitive assay for the detection of ROS formation in cultures of CGNs. Another possibility is that the induced gene products can cope with oxidative stress, without an increase in ROS.

In the lipid peroxidation assay conducted with inducer, to mimic conditions of low grade lipid peroxidation, which may occur amongst other during inflammation, all the four PFAA-containing mixtures accelerated the induced lipid peroxidation, however the Total mixture was by far the most potent. It was the only mixture that had a significant effect at 500x human blood levels. Further, it did also induce the greatest increase in lipid peroxidation at 1000x human levels. This indicates a potential additivity between the different mixture components. In the absence of inducer, the same mixtures (with the exception of the Total mixture) significantly reduced lipid peroxidation as compared to the DMSO control, although the background lipid peroxidation rate was modest. We have previously observed similar findings in CGNs exposed to the single compounds PFOS (10–100 μM) and PFOA (100–600 μM) (Berntsen et al., 2017b). The reduction in lipid peroxidation observed in exposed cells as compared to the controls may potentially be explained by upregulation of antioxidant systems, which fits well with the observed increase in the expression levels of *Prdx6*, *Sod2/3, Gpx1, Hmox1*, *Srxn1* and *Nfe212* genes. In studies using the single compound PFOS, a significant increase in the activity of SOD has been reported after exposure of SH-SY5Y cells (Chen et al., 2014b).

Despite lack of response in the DCF assay and absence of increase in lipid peroxidation without the application of inducers, our results show changes in expression of several genes related to defence against ROS formation or neuroinflammatory processes. One of the most striking results was a strong upregulation of *Prdx6* gene expression level at both 333x and 500x concentrations after exposure to all the mixtures (Supplementary Table S7 and S8). By reducing H_2O_2, peroxynitrite, and organic hydroperoxides (Trujillo et al., 2007), peroxiredoxins (PRDXs) represent a potential major protective barrier against oxidative insults in neurons. PRDX6 is a bifunctional protein that acts as a glutathione peroxidase. Its ability to catalyse the reduction of phospholipid hydroperoxide also suggest that it may have functional roles in phospholipid metabolism in a variety of biological systems (Manevich et al., 2002; Fisher, 2011). Expression of *Prdx6* is suggested to be regulated mainly at the transcriptional level, and can be induced by external stimulation, such as oxidative stress (Shim et al., 2012; Chhunchha et al., 2013). Increased expression level of several other genes at 500x supports the hypothesis that oxidative stress is involved in the POP mixture-induced cell death. Superoxide dismutase 2 and 3 (*Sod2,3*) encoding SOD enzymes playing a role in removal of ROS (Brown-Borg and Rakoczy, 2000), were upregulated after exposure to several of the mixtures, whereas the *Gpx1* gene, encoding glutathione peroxidase 1 (GPx1), showed increased expression after Total mixture exposure. Glutathione peroxidases catalyse the reduction of organic hydroperoxides and hydrogen peroxide by glutathione, and thereby protect cells against oxidative damage. In a recent study, PCB 153 was reported to induce oxidative stress and decreased *GPx1* expression *in vivo* and *in vitro* (Wu et al., 2017a). Alterations in expression levels of *Gstp1* (Glutathione S-Transferase Pi 1), *Gsr* (Glutathione-Disulfide Reductases) and *Gstk1*

(Glutathione S-transferase kappa 1) further support disturbed redox signalling and increased risk for oxidative damage after exposure to both 333x and 500x human blood concentrations of several of the mixtures. Whereas *Gsr* is a gene coding for a central enzyme of cellular antioxidant defence, which reduces oxidised glutathione disulfide (GSSG) to the sulfhydryl form GSH, an important cellular antioxidant, Glutathione S-transferases (GSTs) are a family of enzymes that play an important role in detoxification by catalysing the conjugation of many hydrophobic and electrophilic compounds with reduced glutathione.

Another gene that was downregulated after exposure to the Br mixture at 333x human levels was the Apurinic/Apyrimidinic Endodeoxyribonuclease 1 (*Apex1*) gene, encoding a multifunctional protein that plays a central role in the cellular response to oxidative stress. Recent reports have suggested that the risk for e.g. neurodegeneration in humans following exposure to environmental toxicants is affected by APEX1 alterations in terms of gene-environment interactions (Park et al., 2014).

Also *Sirpa* was found to be strongly upregulated after exposure to both concentrations of all the mixtures. Its gene product, SIRPα, is a transmembrane protein with a key role in the control of phagocytosis (Matozaki et al., 2009), expressed in myeloid cells including microglia (Matozaki et al., 2009; Zhang et al., 2015) as well as in neurons (Toth et al., 2013). Excessive microglial activation may lead to secondary damage and impair CNS repair by releasing harmful substances like nitric oxide, ROS, and proinflammatory cytokines (Hu et al., 2015). SIRPα and CD47 mediate the interplay between microglia and other CNS cells, and are important in neuroinflammatory processes and in several CNS disorders (Zhang et al., 2015). SIRPα has also been shown to be important in the maturation stage of synapse formation *in vivo* and *in vitro* (Ahrens et al., 2009). Upregulation of *Sirpa* expression may therefore be a result of inflammatory processes in the cell culture, and possibly disturbed synapse formation. The latter is supported by downregulation of *Syp* gene, a marker of synaptogenesis. MAPK14 (encoded by *Mapk14*) signalling plays a critical role in astrocyte immune activation (Lo et al., 2014), and the decreased expression of this gene in our study could be a compensatory mechanism for activation of glial cells remaining in the culture.

Heme oxygenase (HMOX) is important for the degradation of heme into biliverdin, carbon monoxide (CO), and iron (Mazurek et al., 2011). Whereas CO acts as a potent vasodilator under normal and stress conditions, biliverdin and its product bilirubin are effective antioxidants. In contrast, freely available cellular iron increases oxidative stress and regulates the expression of many mRNAs (Elbirt and Bonkovsky, 1999; Sorond and Ratan, 2000). There are two isozymes of HMOX: a constitutively expressed heme oxygenase-2 (HMOX2) and an inducible heme oxygenase-1 (HMOX1) (Ryter et al., 2006), where both isoforms catalyse the above reaction. *Hmox1* is highly inducible in response to toxic insults, including exposure to PCBs (Lee et al., 2006), brominated flame retardants (Zou et al., 2013), and perfluorinated compounds (Shi and Zhou, 2010), and is responsive to all types of stimuli that cause oxidative stress (Keyse and Tyrrell, 1989; Stocker, 1990; Dwyer et al., 1992; Hoshida et al., 1996) The strong increased expression level of *Hmox1* in our study by the PFAA-containing mixtures may indicate a protective response against cellular stress, while a decrease in *Hmox2* could result in lowered cellular protection, in line with differently expressed genes coding for redox signaling and inflammatory responses or apoptosis. As an endogenous antioxidant protein, sulfiredoxin1 (SRXN1) can also prevent cellular oxidative stress, as indicated in our cell model. Studies suggest that SRXN1 over-expression protects cells from H_2O_2 induced damage, whereas silencing of *Srxn1* increases sensitivity to oxidative stress (Kang et al., 2005; Vivancos et al., 2005; Li et al., 2013b; Wu et al., 2017b).

Finally, two genes that were upregulated, further supporting oxidative stress as a mechanism after exposure to 500x of the total mixture, and 333x of the Cl + Br mixtures, respectively were *Nfe2l2* and *Nr4a1*. *Nfe2l2* encodes Nuclear factor erythroid 2-related factor 2 (NRF2), a transcription factor controlling basal and induced expression of antioxidant response element-dependent genes regulating the physiological and pathophysiological outcomes of oxidant exposure. NR4A1 (nuclear receptor subfamily 4 group A member 1), a protein encoded by the *Nr4a1* gene, is involved in cell cycle mediation, inflammation and apoptosis (Pei et al., 2006).

Clearly, *Prdx6* is the dominating, discriminantly expressed gene amongst the oxidative stress related genes for all the POPs mixtures at 500x blood levels, as well as for the Total mixture, but not for the Cl + PFAA at 333x blood levels (Table 2). *Sirpa* is furthermore strongly upregulated for all mixtures at 333 and 500x blood levels, and is also among the top discriminantly expressed genes, with the exception of Cl + PFAA at 333x blood levels. In contrast, this gene does not appear as a determinant for the top enriched IPA canonical pathways, which could perhaps be due to its multifunctional role. On the other hand, as shown by the multivariate (OPLS-DA) data analysis, several oxidative stress related genes are differentially expressed for all treatments versus the DMSO control (Table 2), in all sub-mixtures except Cl and Cl + Br (shown by the IPA analysis, Table 3), strongly indicating that disturbed redox processes (including the NRF2-mediated oxidative stress response) are key elements in the toxicity pathways of these human relevant POPs. Interestingly, amongst the enriched canonical pathways shown by the IPA analysis, oxidative stress shows up as an important mechanism of action for all PFAA containing mixtures including Total mixture, while PFAA or Cl alone show a weak and no response, respectively. This could indicate an additive effect between PFAAs and the other halogenated sub-mixtures when it comes to redox responses. Altogether, our data show that POPs are likely to induce oxidative stress responses, with *Prdx6* as the most important driver among the discriminantly expressed genes.

4.4. Mixture-induced effects on oestrogen receptors and synaptic protein expression

On a general basis many agonists are known to downregulate, whereas antagonists upregulate their receptors. Upregulation of oestrogen receptor 2 gene (*Esr2*) in our cell system could thus be a result of anti-oestrogenic activity of the POP mixture. Since oestrogen signalling is also responsible for the growth and maintenance of the nervous system, increased expression level of *Esr2* gene in our cell model may be a compensatory protective mechanism after POP exposure. In addition to its ability to bind to aldosterone, the G-protein coupled oestrogen receptor 1 (GPER1), is recognised as a receptor for oestrogen (Waghulde et al., 2018). In line with increased *Esr2* gene expression level, an increase in *Gper1* gene expression level was observed after exposure to the Total mixture, supporting that the POPs may lead to disturbed oestrogen signalling.

Our results show a reduction in the expression levels of the *Snap25* and *Stxbp1* genes. Synaptosomal-associated protein 25 kDa (SNAP-25), encoded by *Snap25* is an important component of neural soluble N-ethylmaleimide-sensitive factor attachment protein receptor complexes, which are responsible for the Ca^{2+}-dependent exocytosis of neurotransmitters. SNAP-25 is localised exclusively in the presynaptic terminals (Noor and Zahid, 2017), and is used as a marker of synaptogenesis or degeneration of presynaptic terminals (Hossain et al., 2016). Syntaxin binding protein 1 (STXBP1), encoded by *Stxbp1* is also an essential protein for presynaptic vesicle release, and the gene is shown to be highly expressed in rat cerebellum (Swanson et al., 1998). Our results may thus indicate that POP exposure alter the number of synapses, possibly due to apoptotic processes and/or decreased synapse density.

The *Dcx* gene encoded protein appears to direct neuronal migration by regulating the organisation and stability of microtubules, possibly as part of a Ca^{2+}-dependent signal transduction pathway (Slepak et al., 2012). Dysregulation of this gene may cause abnormal migration of neurons during development leading to abnormal neuron positioning and brain malformations (Moffat et al., 2015). In one study decaBDE

exposure resulted in decreased levels of the *Dcx* gene and synaptic proteins in hippocampal neuron cultures (Mariani et al., 2015), which is in line with the reduced expression level of the *Dcx* gene at 333x in our CGNs after exposure to several of the mixtures.

The OPLS-DA analysis shows that the genes coding for oestrogen receptors (*Esr2* and/or *Gper1*) are among the most discriminantly expressed genes in all mixtures with the exception of the Cl + PFAA and Cl + Br mixtures (Table 2). Furthermore, although none of these genes appear in the top enriched IPA canonical pathways (Table 3), *Esr2* and/or *Gper1* seem to be significantly up-regulated after exposure to several of the sub-mixtures as well as the Total mixture at both 500 and 333x blood levels (Supplementary Table S7 and S8). As a result, our data altogether therefore support disturbed oestrogen signalling as a mechanism of action for POP-induced toxicity. None of the genes coding for synaptic proteins and/or synapse function (*Snap25*, *Stxbp1, Syp)*, or *Dcx* appear to be determinants for enriched IPA canonical pathways, and since they do not come up among the most discriminantly expressed genes for the Total-, Cl + PFAA, or Cl + Br mixtures, it appears that these genes may not be the most important drivers for the POP-induced toxicity.

4.5. Mixture-induced effects on developmental and cognitive processes

In the present study we observed downregulation of two genes important for cerebellar development (*Pax6* and *Grin2b*) in CGNs exposed to 500x human blood levels of the combined Br + PFAA and Cl + PFAA mixtures. Interestingly, *Pax6* was also downregulated after exposure to the Cl mixture, although no toxicity accompanied this decrease in expression level. It has been shown that loss of *Grin2b* in hippocampal interneurons reduces glutamate synapse numbers (Kelsch et al., 2014) and its contribution to the regulated Ca^{2+} permeability of the NMDA receptor is crucial in sensing activity-dependent processes (Bliss and Collingridge, 1993; Hu et al., 2016). Interestingly, it also plays a role in cell survival and cell death (Cull-Candy et al., 2001; Endele et al., 2010). The reduction in the expression level of *Grin2b* observed in our study at 500x human blood levels may therefore potentially be involved in the POP-induced loss of cell viability. Interestingly, the fact that effects on *Grin2b* expression level seemed to be dependent on concentration, supports such an involvement, as we in cells treated with the sub-toxic concentration of the mixtures (333x human blood levels) observed no such effect. On the contrary, at this level a slight upregulation of the gene occurred, although not statistically significant. Another gene related to glutamatergic function that was significantly downregulated at 333x human blood levels, here after Br mixture exposure, was the *Grm4* (Glutamate Metabotropic Receptor 4) gene, encoding G protein-coupled receptors linked to the inhibition of the cyclic AMP cascade via decreased adenylate cyclase activity. Metabotropic glutamate receptors (mGluRs) modulate dopaminergic, GABAergic, serotonergic, as well as glutamatergic neurotransmission (Lopez et al., 2014).

Mapk8ip2 encodes C-Jun-amino-terminal kinase-interacting protein 2, which is highly expressed in the brain. This protein is reported to regulate the ratio of AMPA receptors to NMDA receptors at glutamate synapses (Giza et al., 2010). It has furthermore been shown that mice with absence of MAPK8IP2 have abnormal dendritic morphology, as well as motor and cognitive deficits (Giza et al., 2010). Downregulation of *Mapk8ip2* gene after exposure to Br + PFAA and Cl + PFAA mixture may indicate dysregulated glutamate receptor signalling in the CGN culture. Ca^{2+}/calmodulin-dependent protein kinase II (CaMK II) (encoded by *Camk2*) is a downstream activator of the NMDA-R, and is important for learning and memory processes (Wang and Peng, 2016).

Genes related to learning and memory processes in addition to neurodevelopmental processes (*Grin2b, Pax6, Grm4, Mapk8ip2, or Camk2)* are amongst the most discriminantly expressed genes for the Total mixture at 333x blood levels and the Cl + PFAA mixture both at 333 and 500x blood levels, respectively, in addition to Br + PFAA and Br mixtures at 500x blood levels (Table 2). This support the hypothesis that exposure to POPs may disturb learning and memory processes. Despite the reported predominance of the NMDA-R subunit Glu2A in CGNs at DIV 8, we did not observe significant effects on *Grin2a* gene expression levels after exposure to any of the mixtures in the present study. However, for the OPLS-DA models at 333x, *Grin2a* showed up as one of the most discriminantly expressed genes for the Cl + PFAA mixture (Table 2).

Downregulation of the *Pax6* and *Grin2b* expression may result in a decrease in protein levels. When CD-1 mice were exposed via their mothers for six weeks through gestation and lactation to a mixture of the same 29 compounds as included in the Total mixture, effects on PAX6 and GluN2B protein expression in the cerebellum were observed, supporting the effects on genes expression observed in the cultures of CGNs. In control animals PAX6 levels were found to peak after 7 days and to be significantly lower in animals of 3, 6 and 9 weeks of age. GluN2B levels on the other hand peaked after 3 weeks and decreased thereafter (Fig. 4A, B and C). When PAX6 and GluN2B levels were investigated in control, Low POPs and High POPs animals at 3 weeks of age, PAX6 levels were significantly lower in High POPs animals, whereas GluN2B levels were significantly lower in Low POPs animals as compared to controls (Fig. 4D, E and F). While PAX6 is necessary for correct migration and differentiation of CGNs, the GluN2B NMDA-R subunit has a peak in its expression level during cerebellar development and is responsible for Ca^{2+} influx during granule cell migration (Akazawa et al., 1994; Mancini and Atchison, 2007; Tarnok et al., 2008; Mathisen et al., 2013; Fjelldal et al., 2019). A change in expression pattern of these proteins may indicate a deviation from normal development caused by POP exposure. Interestingly, we also observed a significant reduction in GluN2B protein-levels in chicken cerebellum at ED 17 from eggs injected at ED 14 with PFOS (1 μM), a prominent mixture component (Supplementary Figure S9). Although there are limited previous reports on effects on PAX6 and GluN2B levels after exposure to the POPs used in the current mixtures, changes in their amounts have been reported after exposure to other xenobiotics, supporting that toxicant exposure may have adverse effect on levels of these proteins. E.g. Mathisen et al. (2013) observed increased thickness of the cerebellar EGL as well as PAX6 protein levels in 11 day old mice, maternally exposed to bisphenol A (BPA), potentially indicating retarded migration of neurons from the EGL to the IGL. Further, rats maternally exposed to methimazole exhibited a reduction in PAX6 positive cells in the hippocampus, persisting into adulthood (Shiraki et al., 2012). *Pax6* mRNA expression levels were also significantly altered in the frog *Xenopus laevis* exposed to BPA, chlorpyrifos and methylparaben during embryonic development (San Segundo et al., 2013). For GluN2B, *in utero* exposure to buprenorphine reduced cerebellar GluN2B subunit levels in 14 day old rat pups (Fjelldal et al., 2019), whereas reduced subunit levels, associated with impaired cognitive abilities, were observed in hippocampus of 21 day old rats prenatally exposed to deltametrin (Zhang et al., 2018). Further, prenatal ethanol exposure, reduced GluN2B subunit levels (Brady et al., 2013) whereas chronic benzo[a]pyrene exposure resulted in downregulated hippocampal GluN2B gene levels, both in the hippocampus of adult mice (Zhang et al., 2016). The latter was accompanied by deficits in short-term memory and anxiety-like behaviour (Zhang et al., 2016).

5. Conclusion

In the present study we have shown that the Total mixture, as well as selected PFAA-containing sub-mixtures, constructed based on Scandinavian human blood levels, induce toxicity in rat CGNs at concentrations from 500x human levels and above. The concentrations of individual compounds in the mixtures presently inducing effects are lower than concentrations previously reported in most studies. Higher toxicity of the PFAA-mixture in combination with the Cl/Br or Cl + Br mixtures than of the PFAA mixture alone, indicate a degree of additivity

between the mixtures. This is supported by the results from the lipid peroxidation assay, conducted under conditions mimicking low grade inflammation, where the Total mixture was most potent in terms of increasing lipid peroxidation. The cytotoxicity induced in CGN cultures by the PFAA-containing mixtures seems to involve over-activation of NMDA-Rs, confirming previous findings using PFOS. Gene expression studies show significant effects on more genes at the marginally cytotoxic concentration (500x human blood levels), than after exposure to the non-cytotoxic concentration (333x human blood levels). Strong upregulation of *Prdx6* gene expression after exposure to both concentrations of all the mixtures, suggests involvement of oxidative stress after POP exposure, which is supported by the differential expression of several other oxidative stress-related genes. Mixture-induced downregulation of *Pax6* and *Grin2b* in the CGN cultures, two genes important for cerebellar development, as well as reduction in cerebellar PAX6 and GluN2B protein levels after *in utero*/lactational exposure to a mixture containing the same 29 compounds as in the Total mixture, may suggest of a deviation from normal development.

Funding

This study was funded by the Research Council of Norway [grant numbers 204361/H10, 213076/H10].

CRediT authorship contribution statement

Hanne Friis Berntsen: Conceptualization, Methodology, Formal analysis, Investigation, Writing - original draft, Writing - review & editing, Visualization. **Nur Duale:** Conceptualization, Methodology, Formal analysis, Investigation, Writing - original draft, Writing - review & editing, Visualization. **Cesilie Granum Bjørklund:** Investigation, Writing - review & editing. **Oscar Daniel Rangel-Huerta:** Conceptualization, Methodology, Formal analysis, Writing - review & editing. **Kine Dyrberg:** Investigation, Writing - review & editing. **Tim Hofer:** Conceptualization, Methodology, Formal analysis, Investigation, Writing - review & editing. **Kirsten Rakkestad:** Methodology, Investigation, Writing - review & editing. **Gunn Østby:** Conceptualization, Investigation, Writing - review & editing. **Ruth Halsne:** Conceptualization, Methodology, Writing - review & editing. **Gudrun Boge:** Conceptualization, Methodology, Writing - review & editing. **Ragnhild Elisabeth Paulsen:** Conceptualization, Formal analysis, Writing - original draft, Writing - review & editing. **Oddvar Myhre:** Conceptualization, Methodology, Writing - original draft, Writing - review & editing. **Erik Ropstad:** Conceptualization, Methodology, Writing - review & editing, Funding acquisition.

Declaration of Competing Interest

The authors declare that they have no known competing financial interests or personal relationships that could have appeared to influence the work reported in this paper.

Acknowledgements

The authors wish to thank Ms Mona Gaarder and Ms Judit Fuentes-Lazaro (Department of Pharmacy, University of Oslo) for expert technical assistance with Western blotting.

Appendix A. Supplementary data

Supplementary data to this article can be found online at https://doi.org/10.1016/j.envint.2020.106240.

References

Aarem, J., Brunborg, G., Aas, K.K., Harbak, K., Taipale, M.M., Magnus, P., Knudsen, G.P., Duale, N., 2016. Comparison of blood RNA isolation methods from samples stabilized in Tempus tubes and stored at a large human biobank. BMC Res. Notes 9 (1), 430.

Abreu-Villaca, Y., Levin, E.D., 2017. Developmental neurotoxicity of succeeding generations of insecticides. Environ. Int. 99, 55–77.

Ahrens, L., Siebert, U., Ebinghaus, R., 2009. Total body burden and tissue distribution of polyfluorinated compounds in harbor seals (Phoca vitulina) from the German Bight. Mar. Pollut. Bull. 58 (4), 520–525.

Akashi, K., Kakizaki, T., Kamiya, H., Fukaya, M., Yamasaki, M., Abe, M., Natsume, R., Watanabe, M., Sakimura, K., 2009. NMDA Receptor GluN2B (GluR epsilon 2/NR2B) Subunit Is Crucial for Channel Function, Postsynaptic Macromolecular Organization, and Actin Cytoskeleton at Hippocampal CA3 Synapses. J Neurosci 29 (35), 10869–10882.

Akazawa, C., Shigemoto, R., Bessho, Y., Nakanishi, S., Mizuno, N., 1994. Differential expression of five N-methyl-D-aspartate receptor subunit mRNAs in the cerebellum of developing and adult rats. J. Comp. Neurol. 347 (1), 150–160.

Andersen, C.L., Jensen, J.L., Ørntoft, T.F., 2004. Normalization of Real-Time Quantitative Reverse Transcription-PCR Data: A Model-Based Variance Estimation Approach to Identify Genes Suited for Normalization, Applied to Bladder and Colon Cancer Data Sets. Cancer Res. 64 (15), 5245.

Audinat, E., Lambolez, B., Rossier, J., Crepel, F., 1994. Activity-dependent regulation of N-methyl-D-aspartate receptor subunit expression in rat cerebellar granule cells. Eur. J. Neurosci. 6 (12), 1792–1800.

Austdal, L.P., Bjornstad, S., Mathisen, G.H., Aden, P.K., Mikkola, I., Paulsen, R.E., Rakkestad, K.E., 2016. Glucocorticoid Effects on Cerebellar Development in a Chicken Embryo Model: Exploring Changes in PAX6 and Metalloproteinase-9 After Exposure to Dexamethasone. J. Neuroendocrinol. 28 (12).

Babot, Z., Vilaró, M.T., Suñol, C., 2007. Long-term exposure to dieldrin reduces γ-aminobutyric acid type A and N-methyl-D-aspartate receptor function in primary cultures of mouse cerebellar granule cells. J. Neurosci. Res. 85 (16), 3687–3695.

Bell, K.F., Hardingham, G.E., 2011. The influence of synaptic activity on neuronal health. Curr Opin Neurobiol 21 (2), 299–305.

Berntsen, H.F., Berg, V., Thomsen, C., Ropstad, E., Zimmer, K.E., 2017a. The design of an environmentally relevant mixture of persistent organic pollutants for use in in vivo and in vitro studies. J. Toxicol. Environ. Health A 80 (16–18), 1002–1016.

Berntsen, H.F., Bjorklund, C.G., Audinot, J.N., Hofer, T., Verhaegen, S., Lentzen, E., Gutleb, A.C., Ropstad, E., 2017b. Time-dependent effects of perfluorinated compounds on viability in cerebellar granule neurons: Dependence on carbon chain length and functional group attached. Neurotoxicology 63, 70–83.

Berntsen, H.F., Bjorklund, C.G., Strandabo, R., Haug, T.M., Moldes-Anaya, A., Fuentes-Lazaro, J., Verhaegen, S., Paulsen, R.E., Tasker, R.A., Ropstad, E., 2018. PFOS-induced excitotoxicity is dependent on Ca(2+) influx via NMDA receptors in rat cerebellar granule neurons. Toxicol. Appl. Pharmacol. 357, 19–32.

Berntsen, H.F., Wigestrand, M.B., Bogen, I.L., Fonnum, F., Walaas, S.I., Moldes-Anaya, A., 2013. Mechanisms of penitrem-induced cerebellar granule neuron death in vitro: possible involvement of GABAA receptors and oxidative processes. Neurotoxicology 35, 129–136.

Blanco, J., Mulero, M., Lopez, M., Domingo, J.L., Sanchez, D.J., 2011. BDE-99 deregulates BDNF, Bcl-2 and the mRNA expression of thyroid receptor isoforms in rat cerebellar granular neurons. Toxicology 290 (2–3), 305–311.

Bliss, T.V., Collingridge, G.L., 1993. A synaptic model of memory: long-term potentiation in the hippocampus. Nature 361 (6407), 31–39.

Brady, M.L., Diaz, M.R., Iuso, A., Everett, J.C., Valenzuela, C.F., Caldwell, K.K., 2013. Moderate Prenatal Alcohol Exposure Reduces Plasticity and Alters NMDA Receptor Subunit Composition in the Dentate Gyrus. The Journal of Neuroscience 33 (3), 1062.

Brevik, A., Lindeman, B., Rusnakova, V., Olsen, A.-K., Brunborg, G., Duale, N., 2012. Paternal benzo[a]pyrene exposure affects gene expression in the early developing mouse embryo. Toxicological sciences : an official journal of the Society of Toxicology 129 (1), 157–165.

Brown-Borg, H.M., Rakoczy, S.G., 2000. Catalase expression in delayed and premature aging mouse models. Exp Gerontol 35 (2), 199–212.

Brunet, A., Bonni, A., Zigmond, M.J., Lin, M.Z., Juo, P., Hu, L.S., Anderson, M.J., Arden, K.C., Blenis, J., Greenberg, M.E., 1999. Akt promotes cell survival by phosphorylating and inhibiting a Forkhead transcription factor. Cell 96 (6), 857–868.

Cai, J., Yang, J., Jones, D.P., 1998. Mitochondrial control of apoptosis: the role of cytochrome c. Biochim. Biophys. Acta 1366 (1–2), 139–149.

Cebers, G., Cebere, A., Kovacs, A.D., Hogberg, H., Moreira, T., Liljequist, S., 2001. Increased ambient glutamate concentration alters the expression of NMDA receptor subunits in cerebellar granule neurons. Neurochem. Int. 39 (2), 151–160.

Chen, A., Yolton, K., Rauch, S.A., Webster, G.M., Hornung, R., Sjodin, A., Dietrich, K.N., Lanphear, B.P., 2014a. Prenatal polybrominated diphenyl ether exposures and neurodevelopment in U.S. children through 5 years of age: the HOME study. Environ. Health Perspect. 122 (8), 856–862.

Chen, M.H., Ha, E.H., Liao, H.F., Jeng, S.F., Su, Y.N., Wen, T.W., Lien, G.W., Chen, C.Y., Hsieh, W.S., Chen, P.C., 2013. Perfluorinated compound levels in cord blood and neurodevelopment at 2 years of age. Epidemiology 24 (6), 800–808.

Chen, N., Li, J., Li, D., Yang, Y., He, D., 2014b. Chronic exposure to perfluorooctane sulfonate induces behavior defects and neurotoxicity through oxidative damages, in vivo and in vitro. PLoS One 9 (11), e113453.

Chhunchha, B., Fatma, N., Kubo, E., Rai, P., Singh, S.P., Singh, D.P., 2013. Curcumin abates hypoxia-induced oxidative stress based-ER stress-mediated cell death in

mouse hippocampal cells (HT22) by controlling Prdx6 and NF-kappaB regulation. Am J Physiol Cell Physiol 304 (7), C636–C655.
Choi, S.A., Kim, S.J., Chung, K.C., 2006. Huntingtin-interacting protein 1-mediated neuronal cell death occurs through intrinsic apoptotic pathways and mitochondrial alterations. Febs Lett 580 (22), 5275–5282.
Cull-Candy, S., Brickley, S., Farrant, M., 2001. NMDA receptor subunits: diversity, development and disease. Curr. Opin. Neurobiol. 11 (3), 327–335.
Dewailly, E., Mulvad, G., Pedersen, H.S., Ayotte, P., Demers, A., Weber, J.P., Hansen, J. C., 1999. Concentration of organochlorines in human brain, liver, and adipose tissue autopsy samples from Greenland. Environ. Health Perspect. 107 (10), 823–828.
Dreiem, A., Rykken, S., Lehmler, H.J., Robertson, L.W., Fonnum, F., 2009. Hydroxylated polychlorinated biphenyls increase reactive oxygen species formation and induce cell death in cultured cerebellar granule cells. Toxicol. Appl. Pharmacol. 240 (2), 306–313.
Duale, N., Brunborg, G., Rønningen, K.S., Briese, T., Aarem, J., Aas, K.K., Magnus, P., Stoltenberg, C., Susser, E., Lipkin, W.I., 2012. Human blood RNA stabilization in samples collected and transported for a large biobank. BMC Res. Notes 5, 510–510.
Duale, N., Lipkin, W.I., Briese, T., Aarem, J., Rønningen, K.S., Aas, K.K., Magnus, P., Harbak, K., Susser, E., Brunborg, G., 2014a. Long-term storage of blood RNA collected in RNA stabilizing Tempus tubes in a large biobank–evaluation of RNA quality and stability. BMC Res. Notes 7,, 633–633.
Duale, N., Olsen, A.K., Christensen, T., Butt, S.T., Brunborg, G., 2010. Octyl methoxycinnamate modulates gene expression and prevents cyclobutane pyrimidine dimer formation but not oxidative DNA damage in UV-exposed human cell lines. Toxicol. Sci. 114 (2), 272–284.
Duale, N., Steffensen, I.L., Andersen, J., Brevik, A., Brunborg, G., Lindeman, B., 2014b. Impaired sperm chromatin integrity in obese mice. Andrology 2 (2), 234–243.
Dwyer, B.E., Nishimura, R.N., Devellis, J., Yoshida, T., 1992. Heme Oxygenase Is a Heat-Shock Protein and Pest Protein in Rat Astroglial Cells. Glia 5 (4), 300–305.
Elbirt, K.K., Bonkovsky, H.L., 1999. Heme oxygenase: recent advances in understanding its regulation and role. Proc. Assoc. Am. Physicians 111 (5), 438–447.
Endele, S., Rosenberger, G., Geider, K., Popp, B., Tamer, C., Stefanova, I., Milh, M., Kortum, F., Fritsch, A., Pientka, F.K., Hellenbroich, Y., Kalscheuer, V.M., Kohlhase, J., Moog, U., Rappold, G., Rauch, A., Ropers, H.H., von Spiczak, S., Tonnies, H., Villeneuve, N., Villard, L., Zabel, B., Zenker, M., Laube, B., Reis, A., Wieczorek, D., Van Maldergem, L., Kutsche, K., 2010. Mutations in GRIN2A and GRIN2B encoding regulatory subunits of NMDA receptors cause variable neurodevelopmental phenotypes. Nat Genet 42 (11), 1021–1026.
Engelkamp, D., Rashbass, P., Seawright, A., van Heyningen, V., 1999. Role of Pax6 in development of the cerebellar system. Development 126 (16), 3585–3596.
Eskenazi, B., Chevrier, J., Rauch, S.A., Kogut, K., Harley, K.G., Johnson, C., Trujillo, C., Sjodin, A., Bradman, A., 2013. In utero and childhood polybrominated diphenyl ether (PBDE) exposures and neurodevelopment in the CHAMACOS study. Environ. Health Perspect. 121 (2), 257–262.
Espinosa, J.S., Wheeler, D.G., Tsien, R.W., Luo, L., 2009. Uncoupling dendrite growth and patterning: single-cell knockout analysis of NMDA receptor 2B. Neuron 62 (2), 205–217.
Fan, T.J., Han, L.H., Cong, R.S., Liang, J., 2005. Caspase family proteases and apoptosis. Acta Biochim Biophys Sin (Shanghai) 37 (11), 719–727.
Fisher, A.B., 2011. Peroxiredoxin 6: a bifunctional enzyme with glutathione peroxidase and phospholipase A(2) activities. Antioxid Redox Signal 15 (3), 831–844.
Fisher, M., Arbuckle, T.E., Liang, C.L., LeBlanc, A., Gaudreau, E., Foster, W.G., Haines, D., Davis, K., Fraser, W.D., 2016. Concentrations of persistent organic pollutants in maternal and cord blood from the maternal-infant research on environmental chemicals (MIREC) cohort study. Environ. Health 15 (1), 59.
Fjelldal, M.F., Hadera, M.G., Kongstorp, M., Austdal, L.P.E., Sulovic, A., Andersen, J.M., Paulsen, R.E., 2019. Opioid receptor-mediated changes in the NMDA receptor in developing rat and chicken. Int. J. Dev. Neurosci. 78, 19–27.
Fonnum, F., Mariussen, E., 2009. Mechanisms involved in the neurotoxic effects of environmental toxicants such as polychlorinated biphenyls and brominated flame retardants. J. Neurochem. 111 (6), 1327–1347.
Freberg, B.I., Haug, L.S., Olsen, R., Daae, H.L., Hersson, M., Thomsen, C., Thorud, S., Becher, G., Molander, P., Ellingsen, D.G., 2010. Occupational Exposure to Airborne Perfluorinated Compounds during Professional Ski Waxing. Environ. Sci. Technol. 44 (19), 7723–7728.
Fu, J., Gao, Y., Cui, L., Wang, T., Liang, Y., Qu, G., Yuan, B., Wang, Y., Zhang, A., Jiang, G., 2016. Occurrence, temporal trends, and half-lives of perfluoroalkyl acids (PFAAs) in occupational workers in China. Sci. Rep. 6, 38039.
Gallo, V., Ciotti, M.T., Coletti, A., Aloisi, F., Levi, G., 1982. Selective release of glutamate from cerebellar granule cells differentiating in culture. Proc. Natl. Acad. Sci. U. S. A. 79 (24), 7919–7923.
Gallo, V., Kingsbury, A., Balazs, R., Jorgensen, O.S., 1987. The role of depolarization in the survival and differentiation of cerebellar granule cells in culture. J. Neurosci. 7 (7), 2203–2213.
Gascon, M., Vrijheid, M., Martinez, D., Forns, J., Grimalt, J.O., Torrent, M., Sunyer, J., 2011. Effects of pre and postnatal exposure to low levels of polybromodiphenyl ethers on neurodevelopment and thyroid hormone levels at 4 years of age. Environ. Int. 37 (3), 605–611.
Gerschutz, A., Heinsen, H., Grunblatt, E., Wagner, A.K., Bartl, J., Meissner, C., Fallgatter, A.J., Al-Sarraj, S., Troakes, C., Ferrer, I., Arzberger, T., Deckert, J., Riederer, P., Fischer, M., Tatschner, T., Monoranu, C.M., 2014. Neuron-specific alterations in signal transduction pathways associated with Alzheimer's disease. J. Alzheimers Dis. 40 (1), 135–142.
Giza, J., Urbanski, M.J., Prestori, F., Bandyopadhyay, B., Yam, A., Friedrich, V., Kelley, K., D'Angelo, E., Goldfarb, M., 2010. Behavioral and cerebellar transmission deficits in mice lacking the autism-linked gene islet brain-2. The Journal of neuroscience : the official journal of the Society for Neuroscience 30 (44), 14805–14816.
Gutzkow, K.B., Duale, N., Danielsen, T., von Stedingk, H., Shahzadi, S., Instanes, C., Olsen, A.-K., Steffensen, I.-L., Hofer, T., Törnqvist, M., Brunborg, G., Lindeman, B., 2016. Enhanced susceptibility of obese mice to glycidamide-induced sperm chromatin damage without increased oxidative stress. 4 (6), 1102–1114.
Harris, M.H., Oken, E., Rifas-Shiman, S.L., Calafat, A.M., Ye, X., Bellinger, D.C., Webster, T.F., White, R.F., Sagiv, S.K., 2018. Prenatal and childhood exposure to per- and polyfluoroalkyl substances (PFASs) and child cognition. Environ. Int. 115, 358–369.
Hendriks, H.S., Westerink, R.H., 2015. Neurotoxicity and risk assessment of brominated and alternative flame retardants. Neurotoxicol. Teratol. 52 (Pt B), 248–269.
Hitomi, J., Katayama, T., Eguchi, Y., Kudo, T., Taniguchi, M., Koyama, Y., Manabe, T., Yamagishi, S., Bando, Y., Imaizumi, K., Tsujimoto, Y., Tohyama, M., 2004. Involvement of caspase-4 in endoplasmic reticulum stress-induced apoptosis and Abeta-induced cell death. J Cell Biol 165 (3), 347–356.
Hofer, T., Jorgensen, T.O., Olsen, R.L., 2014. Comparison of food antioxidants and iron chelators in two cellular free radical assays: strong protection by luteolin. J. Agric. Food Chem. 62 (33), 8402–8410.
Hoffman, K., Adgent, M., Goldman, B.D., Sjodin, A., Daniels, J.L., 2012. Lactational exposure to polybrominated diphenyl ethers and its relation to social and emotional development among toddlers. Environ. Health Perspect. 120 (10), 1438–1442.
Hoshida, S., Nishida, M., Yamashita, N., Igarashi, J., Aoki, K., Hori, M., Kuzuya, T., Tada, M., 1996. Heme oxygenase-1 expression and its relation to oxidative stress during primary culture of cardiomyocytes. J Mol Cell Cardiol 28 (9), 1845–1855.
Hossain, S., Bhowmick, S., Jahan, S., Rozario, L., Sarkar, M., Islam, S., Basunia, M.A., Rahman, A., Choudhury, B.K., Shahjalal, H., 2016. Maternal lead exposure decreases the levels of brain development and cognition-related proteins with concomitant upsurges of oxidative stress, inflammatory response and apoptosis in the offspring rats. Neurotoxicology 56, 150–158.
Hoyer, B.B., Ramlau-Hansen, C.H., Obel, C., Pedersen, H.S., Hernik, A., Ogniev, V., Jonsson, B.A., Lindh, C.H., Rylander, L., Rignell-Hydbom, A., Bonde, J.P., Toft, G., 2015. Pregnancy serum concentrations of perfluorinated alkyl substances and offspring behaviour and motor development at age 5–9 years–a prospective study. Environ. Health 14, 2.
Hu, C., Chen, W., Myers, S.J., Yuan, H., Traynelis, S.F., 2016. Human GRIN2B variants in neurodevelopmental disorders. J. Pharmacol. Sci. 132 (2), 115–121.
Hu, X., Leak, R.K., Shi, Y., Suenaga, J., Gao, Y., Zheng, P., Chen, J., 2015. Microglial and macrophage polarization-new prospects for brain repair. Nat Rev Neurol 11 (1), 56–64.
Hudecova, A.M., Hansen, K.E.A., Mandal, S., Berntsen, H.F., Khezri, A., Bale, T.L., Fraser, T.W.K., Zimmer, K.E., Ropstad, E., 2018. A human exposure based mixture of persistent organic pollutants affects the stress response in female mice and their offspring. Chemosphere 197, 585–593.
Imai, Y., Kimura, T., Murakami, A., Yajima, N., Sakamaki, K., Yonehara, S., 1999. The CED-4-homologous protein FLASH is involved in Fas-mediated activation of caspase-8 during apoptosis. Nature 398 (6730), 777–785.
Imaizumi, K., Miyoshi, K., Katayama, T., Yoneda, T., Taniguchi, M., Kudo, T., Tohyama, M., 2001. The unfolded protein response and Alzheimer's disease. Biochim Biophys Acta 1536 (2–3), 85–96.
Swerea, I.V.F., 2009. Survey, screening and analyses of PFCs in consumer products. Mölndal, Sweden.
Jacobs, C.M., Aden, P., Mathisen, G.H., Khuong, E., Gaarder, M., Loberg, E.M., Lomo, J., Maehlen, J., Paulsen, R.E., 2006. Chicken cerebellar granule neurons rapidly develop excitotoxicity in culture. J. Neurosci. Methods 156 (1–2), 129–135.
Kang, K.W., Lee, S.J., Kim, S.G., 2005. Molecular mechanism of nrf2 activation by oxidative stress. Antioxid Redox Signal 7 (11–12), 1664–1673.
Karrman, A., Ericson, I., van Bavel, B., Darnerud, P.O., Aune, M., Glynn, A., Lignell, S., Lindstrom, G., 2007. Exposure of perfluorinated chemicals through lactation: levels of matched human milk and serum and a temporal trend, 1996–2004. Sweden. Environ. Health Perspect. 115 (2), 226–230.
Karrman, A., van Bavel, B., Jarnberg, U., Hardell, L., Lindstrom, G., 2006. Perfluorinated chemicals in relation to other persistent organic pollutants in human blood. Chemosphere 64 (9), 1582–1591.
Kelsch, W., Li, Z., Wieland, S., Senkov, O., Herb, A., Gongrich, C., Monyer, H., 2014. GluN2B-containing NMDA receptors promote glutamate synapse development in hippocampal interneurons. J Neurosci 34 (48), 16022–16030.
Keyse, S.M., Tyrrell, R.M., 1989. Heme Oxygenase Is the Major 32-Kda Stress Protein-Induced in Human-Skin Fibroblasts by Uva Radiation, Hydrogen-Peroxide, and Sodium Arsenite. P Natl Acad Sci USA 86 (1), 99–103.
Khezri, A., Fraser, T.W., Nourizadeh-Lillabadi, R., Kamstra, J.H., Berg, V., Zimmer, K.E., Ropstad, E., 2017. A Mixture of Persistent Organic Pollutants and Perfluorooctanesulfonic Acid Induces Similar Behavioural Responses, but Different Gene Expression Profiles in Zebrafish Larvae. Int. J. Mol. Sci. 18 (2).
Kluck, R.M., Bossy-Wetzel, E., Green, D.R., Newmeyer, D.D., 1997. The release of cytochrome c from mitochondria: a primary site for Bcl-2 regulation of apoptosis. Science 275 (5303), 1132–1136.
Kodavanti, P.R., Ward, T.R., 1998. Interactive effects of environmentally relevant polychlorinated biphenyls and dioxins on [3H]phorbol ester binding in rat cerebellar granule cells. Environ. Health Perspect. 106 (8), 479–486.
Kodavanti, P.R., Ward, T.R., Ludewig, G., Robertson, L.W., Birnbaum, L.S., 2005. Polybrominated diphenyl ether (PBDE) effects in rat neuronal cultures: 14C-PBDE accumulation, biological effects, and structure-activity relationships. Toxicol. Sci. 88 (1), 181–192.

Kodavanti, P.R.S., 2006. Neurotoxicity of persistent organic pollutants: possible mode(s) of action and further considerations. Dose-response : a publication of International Hormesis Society 3 (3), 273–305.
Kotthoff, M., Muller, J., Jurling, H., Schlummer, M., Fiedler, D., 2015. Perfluoroalkyl and polyfluoroalkyl substances in consumer products. Environ. Sci. Pollut. Res. Int. 22 (19), 14546–14559.
Lau, C., 2012. Perfluorinated compounds, in: Luch, A. (Ed.) Molecular, clinical and environmental toxicology. Volume 3: Environmental Toxicology. Springer Basel, Basel, pp. 47-86.
Lee, D.W., Gelein, R.M., Opanashuk, L.A., 2006. Heme-oxygenase-1 promotes polychlorinated biphenyl mixture aroclor 1254-induced oxidative stress and dopaminergic cell injury. Toxicol Sci 90 (1), 159–167.
Lee, H.G., Lee, Y.J., Yang, J.H., 2012. Perfluorooctane sulfonate induces apoptosis of cerebellar granule cells via a ROS-dependent protein kinase C signaling pathway. Neurotoxicology 33 (3), 314–320.
Lenters, V., Iszatt, N., Forns, J., Čechová, E., Kočan, A., Legler, J., Leonards, P., Stigum, H., Eggesbø, M., 2019. Early-life exposure to persistent organic pollutants (OCPs, PBDEs, PCBs, PFASs) and attention-deficit/hyperactivity disorder: A multi-pollutant analysis of a Norwegian birth cohort. Environ. Int. 125, 33–42.
Li, L.X., Chen, L., Meng, X.Z., Chen, B.H., Chen, S.Q., Zhao, Y., Zhao, L.F., Liang, Y., Zhang, Y.H., 2013a. Exposure levels of environmental endocrine disruptors in mother-newborn pairs in China and their placental transfer characteristics. PLoS One 8 (5), e62526.
Li, Q., Yu, S., Wu, J., Zou, Y., Zhao, Y., 2013b. Sulfiredoxin-1 protects PC12 cells against oxidative stress induced by hydrogen peroxide. J Neurosci Res 91 (6), 861–870.
Livak, K.J., Schmittgen, T.D., 2001. Analysis of relative gene expression data using real-time quantitative PCR and the 2(-Delta Delta C(T)) Method. Methods 25 (4), 402–408.
Llansola, M., Sanchez-Perez, A., Cauli, O., Felipo, V., 2005. Modulation of NMDA receptors in the cerebellum. 1. Properties of the NMDA receptor that modulate its function. Cerebellum (London, England) 4 (3), 154–161.
Lo, U., Selvaraj, V., Plane, J.M., Chechneva, O.V., Otsu, K., Deng, W., 2014. p38 alpha (MAPK14) critically regulates the immunological response and the production of specific cytokines and chemokines in astrocytes. Sci Rep-Uk 4.
Lopez, J.P., Lim, R., Cruceanu, C., Crapper, L., Fasano, C., Labonte, B., Maussion, G., Yang, J.P., Yerko, V., Vigneault, E., El Mestikawy, S., Mechawar, N., Pavlidis, P., Turecki, G., 2014. miR-1202 is a primate-specific and brain-enriched microRNA involved in major depression and antidepressant treatment. Nat. Med. 20 (7), 764–768.
Lu, X., Li, Y., Wang, W., Chen, S., Liu, T., Jia, D., Quan, X., Sun, D., Chang, A.K., Gao, B., 2014. 3 β-hydroxysteroid-Δ 24 reductase (DHCR24) protects neuronal cells from apoptotic cell death induced by endoplasmic reticulum (ER) stress. PLoS One 9 (1) e86753–e86753.
Maekawa, M., Iwayama, Y., Nakamura, K., Sato, M., Toyota, T., Ohnishi, T., Yamada, K., Miyachi, T., Tsujii, M., Hattori, E., Maekawa, N., Osumi, N., Mori, N., Yoshikawa, T., 2009. A novel missense mutation (Leu46Val) of PAX6 found in an autistic patient. Neurosci. Lett. 462 (3), 267–271.
Maestri, L., Negri, S., Ferrari, M., Ghittori, S., Fabris, F., Danesino, P., Imbriani, M., 2006. Determination of perfluorooctanoic acid and perfluorooctanesulfonate in human tissues by liquid chromatography/single quadrupole mass spectrometry. Rapid Commun. Mass Spectrom. 20 (18), 2728–2734.
Mamsen, L.S., Bjorvang, R.D., Mucs, D., Vinnars, M.T., Papadogiannakis, N., Lindh, C.H., Andersen, C.Y., Damdimopoulou, P., 2019. Concentrations of perfluoroalkyl substances (PFASs) in human embryonic and fetal organs from first, second, and third trimester pregnancies. Environ. Int. 124, 482–492.
Mancini, J.D., Atchison, W.D., 2007. The NR2B subunit in NMDA receptors is functionally important during cerebellar granule cell migration. Neurosci. Lett. 429 (2–3), 87–90.
Manevich, Y., Sweitzer, T., Pak, J.H., Feinstein, S.I., Muzykantov, V., Fisher, A.B., 2002. 1-Cys peroxiredoxin overexpression protects cells against phospholipid peroxidation-mediated membrane damage. Proc Natl Acad Sci U S A 99 (18), 11599–11604.
Manoli, I., Alesci, S., Blackman, M.R., Su, Y.A., Rennert, O.M., Chrousos, G.P., 2007. Mitochondria as key components of the stress response. Trends Endocrinol. Metab. 18 (5), 190–198.
Mariani, A., Fanelli, R., Re Depaolini, A., De Paola, M., 2015. Decabrominated diphenyl ether and methylmercury impair fetal nervous system development in mice at documented human exposure levels. Dev. Neurobiol. 75 (1), 23–38.
Mariussen, E., 2012. Neurotoxic effects of perfluoroalkylated compounds: mechanisms of action and environmental relevance. Arch. Toxicol. 86 (9), 1349–1367.
Mariussen, E., Fonnum, F., 2001. The effect of polychlorinated biphenyls on the high affinity uptake of the neurotransmitters, dopamine, serotonin, glutamate and GABA, into rat brain synaptosomes. Toxicology 159 (1), 11–21.
Mariussen, E., Myhre, O., Reistad, T., Fonnum, F., 2002. The polychlorinated biphenyl mixture aroclor 1254 induces death of rat cerebellar granule cells: the involvement of the N-methyl-D-aspartate receptor and reactive oxygen species. Toxicol. Appl. Pharmacol. 179 (3), 137–144.
Markham, A., Bains, R., Franklin, P., Spedding, M., 2014. Changes in mitochondrial function are pivotal in neurodegenerative and psychiatric disorders: how important is BDNF? Br. J. Pharmacol. 171 (8), 2206–2229.
Mathisen, G.H., Yazdani, M., Rakkestad, K.E., Aden, P.K., Bodin, J., Samuelsen, M., Nygaard, U.C., Goverud, I.L., Gaarder, M., Loberg, E.M., Bolling, A.K., Becher, R., Paulsen, R.E., 2013. Prenatal exposure to bisphenol A interferes with the development of cerebellar granule neurons in mice and chicken. Int. J. Dev. Neurosci. 31 (8), 762–769.
Matozaki, T., Murata, Y., Okazawa, H., Ohnishi, H., 2009. Functions and molecular mechanisms of the CD47-SIRPalpha signalling pathway. Trends Cell Biol 19 (2), 72–80.
Mattson, M.P., 2008. Glutamate and neurotrophic factors in neuronal plasticity and disease. Ann. N. Y. Acad. Sci. 1144, 97–112.
Mazurek, B., Amarjargal, N., Haupt, H., Fuchs, J., Olze, H., Machulik, A., Gross, J., 2011. Expression of genes implicated in oxidative stress in the cochlea of newborn rats. Hear. Res. 277 (1–2), 54–60.
Metzler, M., Gan, L., Wong, T.P., Liu, L., Helm, J., Liu, L., Georgiou, J., Wang, Y., Bissada, N., Cheng, K., Roder, J.C., Wang, Y.T., Hayden, M.R., 2007. NMDA receptor function and NMDA receptor-dependent phosphorylation of huntingtin is altered by the endocytic protein HIP1. J Neurosci 27 (9), 2298–2308.
Mishra, N., Kouzmitcheva, E., Orsino, A., Minassian, B.A., 2016. Chromosome 12p Deletion Spanning the GRIN2B Gene Presenting With a Neurodevelopmental Phenotype: A Case Report and Review of Literature. Child Neurol Open 3, 2329048X16629980.
Mitchell, M.M., Woods, R., Chi, L.H., Schmidt, R.J., Pessah, I.N., Kostyniak, P.J., LaSalle, J.M., 2012. Levels of select PCB and PBDE congeners in human postmortem brain reveal possible environmental involvement in 15q11-q13 duplication autism spectrum disorder. Environ. Mol. Mutagen. 53 (8), 589–598.
Miyoshi, J., Takai, Y., 2004. Dual role of DENN/MADD (Rab3GEP) in neurotransmission and neuroprotection. Trends Mol. Med. 10 (10), 476–480.
Moffat, J.J., Ka, M., Jung, E.-M., Kim, W.-Y., 2015. Genes and brain malformations associated with abnormal neuron positioning. Mol. Brain 8 (1), 72–72.
Mori, H., Mishina, M., 1995. Structure and function of the NMDA receptor channel. Neuropharmacology 34 (10), 1219–1237.
Myhre, O., Andersen, J.M., Aarnes, H., Fonnum, F., 2003. Evaluation of the probes 2',7'-dichlorofluorescin diacetate, luminol, and lucigenin as indicators of reactive species formation. Biochem. Pharmacol. 65 (10), 1575–1582.
Nicoletti, F., Wroblewski, J.T., Novelli, A., Alho, H., Guidotti, A., Costa, E., 1986. The activation of inositol phospholipid metabolism as a signal-transducing system for excitatory amino acids in primary cultures of cerebellar granule cells. J. Neurosci. 6 (7), 1905–1911.
Nilsson, H., Karrman, A., Westberg, H., Rotander, A., van Bavel, B., Lindstrom, G., 2010. A time trend study of significantly elevated perfluorocarboxylate levels in humans after using fluorinated ski wax. Environ. Sci. Technol. 44 (6), 2150–2155.
Noor, A., Zahid, S., 2017. A review of the role of synaptosomal-associated protein 25 (SNAP-25) in neurological disorders. Int. J. Neurosci. 127 (9), 805–811.
Novelli, A., Henneberry, R.C., 1987. cGmp synthesis in cultured cerebellar neurons is stimulated by glutamate via a Ca2+-mediated, differentiation-dependent mechanism. Brain Res. 431 (2), 307–310.
Ow, Y.P., Green, D.R., Hao, Z., Mak, T.W., 2008. Cytochrome c: functions beyond respiration. Nat. Rev. Mol. Cell Biol. 9 (7), 532–542.
Pan, Y., Chen, J., Guo, H., Ou, J., Peng, Y., Liu, Q., Shen, Y., Shi, L., Liu, Y., Xiong, Z., Zhu, T., Luo, S., Hu, Z., Zhao, J., Xia, K., 2015. Association of genetic variants of GRIN2B with autism. Sci Rep 5, 8296.
Paoletti, P., Bellone, C., Zhou, Q., 2013. NMDA receptor subunit diversity: impact on receptor properties, synaptic plasticity and disease. Nat. Rev. Neurosci. 14 (6), 383–400.
Park, J.S., Kim, H.L., Kim, Y.J., Weon, J.I., Sung, M.K., Chung, H.W., Seo, Y.R., 2014. Human AP endonuclease 1: a potential marker for the prediction of environmental carcinogenesis risk. Oxid. Med. Cell. Longev. 2014, 730301.
Pedraza, N., Rafel, M., Navarro, I., Encinas, M., Aldea, M., Gallego, C., 2009. Mixed lineage kinase phosphorylates transcription factor E47 and inhibits TrkB expression to link neuronal death and survival pathways. J. Biol. Chem. 284 (47), 32980–32988.
Pei, L., Castrillo, A., Tontonoz, P., 2006. Regulation of macrophage inflammatory gene expression by the orphan nuclear receptor Nur77. Mol. Endocrinol. 20 (4), 786–794.
Perez-Gomez, A., Garcia-Rodriguez, A., James, K.J., Ferrero-Gutierrez, A., Novelli, A., Fernandez-Sanchez, M.T., 2004. The marine toxin dinophysistoxin-2 induces differential apoptotic death of rat cerebellar neurons and astrocytes. Toxicol. Sci. 80 (1), 74–82.
Pessah, I.N., Lein, P.J., Seegal, R.F., Sagiv, S.K., 2019. Neurotoxicity of polychlorinated biphenyls and related organohalogens. Acta Neuropathol. 138 (3), 363–387.
Polder, A., Thomsen, C., Lindstrom, G., Loken, K.B., Skaare, J.U., 2008. Levels and temporal trends of chlorinated pesticides, polychlorinated biphenyls and brominated flame retardants in individual human breast milk samples from Northern and Southern Norway. Chemosphere 73 (1), 14–23.
Rakic, P., 1971. Neuron-glia relationship during granule cell migration in developing cerebellar cortex. A Golgi and electronmicroscopic study in Macacus Rhesus. J. Comp. Neurol. 141 (3), 283–312.
Reistad, T., Fonnum, F., Mariussen, E., 2006. Neurotoxicity of the pentabrominated diphenyl ether mixture, DE-71, and hexabromocyclododecane (HBCD) in rat cerebellar granule cells in vitro. Arch. Toxicol. 80 (11), 785–796.
Reistad, T., Fonnum, F., Mariussen, E., 2013. Perfluoroalkylated compounds induce cell death and formation of reactive oxygen species in cultured cerebellar granule cells. Toxicol. Lett. 218 (1), 56–60.
Reistad, T., Mariussen, E., Ring, A., Fonnum, F., 2007. In vitro toxicity of tetrabromobisphenol-A on cerebellar granule cells: cell death, free radical formation, calcium influx and extracellular glutamate. Toxicol. Sci. 96 (2), 268–278.
Roze, E., Meijer, L., Bakker, A., Van Braeckel, K.N., Sauer, P.J., Bos, A.F., 2009. Prenatal exposure to organohalogens, including brominated flame retardants, influences motor, cognitive, and behavioral performance at school age. Environ. Health Perspect. 117 (12), 1953–1958.
Ryter, S.W., Alam, J., Choi, A.M., 2006. Heme oxygenase-1/carbon monoxide: from basic science to therapeutic applications. Physiol. Rev. 86 (2), 583–650.

Saeed, A.I., Bhagabati, N.K., Braisted, J.C., Liang, W., Sharov, V., Howe, E.A., Li, J., Thiagarajan, M., White, J.A., Quackenbush, J., 2006. TM4 microarray software suite. Methods Enzymol. 411, 134–193.
Sagiv, S.K., Kogut, K., Gaspar, F.W., Gunier, R.B., Harley, K.G., Parra, K., Villasenor, D., Bradman, A., Holland, N., Eskenazi, B., 2015. Prenatal and childhood polybrominated diphenyl ether (PBDE) exposure and attention and executive function at 9–12 years of age. Neurotoxicol. Teratol. 52 (Pt B), 151–161.
Sagiv, S.K., Nugent, J.K., Brazelton, T.B., Choi, A.L., Tolbert, P.E., Altshul, L.M., Korrick, S.A., 2008. Prenatal organochlorine exposure and measures of behavior in infancy using the Neonatal Behavioral Assessment Scale (NBAS). Environ. Health Perspect. 116 (5), 666–673.
Sagiv, S.K., Thurston, S.W., Bellinger, D.C., Altshul, L.M., Korrick, S.A., 2012. Neuropsychological measures of attention and impulse control among 8-year-old children exposed prenatally to organochlorines. Environ. Health Perspect. 120 (6), 904–909.
Sagiv, S.K., Thurston, S.W., Bellinger, D.C., Tolbert, P.E., Altshul, L.M., Korrick, S.A., 2010. Prenatal organochlorine exposure and behaviors associated with attention deficit hyperactivity disorder in school-aged children. Am. J. Epidemiol. 171 (5), 593–601.
Salvesen, G.S., 2002. Caspases: opening the boxes and interpreting the arrows. Cell Death Differ. 9 (1), 3–5.
San Segundo, L., Martini, F., Pablos, M.V., 2013. Gene expression responses for detecting sublethal effects of xenobiotics and whole effluents on a Xenopus laevis embryo assay. Environ. Toxicol. Chem. 32 (9), 2018–2025.
Schmahmann, J.D., 2010. The role of the cerebellum in cognition and emotion: personal reflections since 1982 on the dysmetria of thought hypothesis, and its historical evolution from theory to therapy. Neuropsychol. Rev. 20 (3), 236–260.
Schmittgen, T.D., Livak, K.J., 2008. Analyzing real-time PCR data by the comparative C (T) method. Nat. Protoc. 3 (6), 1101–1108.
Schousboe, A., Meier, E., Drejer, J., Hertz, L., 1989. Preparation of cultures of mouse (rat) cerebellar granule cells. In: Shahar, A., de Vellis, J., Vernadakis, A., Haber, B. (Eds.), A Dissection and Tissue Culture Manual for the Nervous System. Liss, New York, A.R, pp. 203–206.
Schramm, M., Eimerl, S., Costa, E., 1990. Serum and depolarizing agents cause acute neurotoxicity in cultured cerebellar granule cells: role of the glutamate receptor responsive to N-methyl-D-aspartate. Proc. Natl. Acad. Sci. U. S. A. 87 (3), 1193–1197.
Scott, A.M., Saleh, M., 2007. The inflammatory caspases: guardians against infections and sepsis. Cell Death Differ 14 (1), 23–31.
Secretariat of the Stockholm convention, 2017. The 16 new POPs. United Nations Environment, Geneva, Switzerland.
Secretariat of the Stockholm Convention, 2019a. The 12 intitial POPs under the Stockholm Convention. http://chm.pops.int/TheConvention/ThePOPs/The12InitialPOPs/tabid/296/Default.aspx (Accessed 18 May 2020).
Secretariat of the Stockholm Convention, 2019b. Chemicals proposed for listing under the Convention. http://chm.pops.int/TheConvention/ThePOPs/ChemicalsProposedforListing/tabid/2510/Default.aspx. (Accessed August 10 2020).
Shi, X., Zhou, B., 2010. The role of Nrf2 and MAPK pathways in PFOS-induced oxidative stress in zebrafish embryos. Toxicol Sci 115 (2), 391–400.
Shim, S.Y., Kim, H.S., Kim, E.K., Choi, J.H., 2012. Expression of peroxiredoxin 1, 2, and 6 in the rat brain during perinatal development and in response to dexamethasone. Free Radic Res 46 (3), 231–239.
Shiraki, A., Akane, H., Ohishi, T., Wang, L., Morita, R., Suzuki, K., Mitsumori, K., Shibutani, M., 2012. Similar distribution changes of GABAergic interneuron subpopulations in contrast to the different impact on neurogenesis between developmental and adult-stage hypothyroidism in the hippocampal dentate gyrus in rats. Arch. Toxicol. 86 (10), 1559–1569.
Slepak, T.I., Salay, L.D., Lemmon, V.P., Bixby, J.L., 2012. Dyrk kinases regulate phosphorylation of doublecortin, cytoskeletal organization, and neuronal morphology. Cytoskeleton (Hoboken, N.J.) 69 (7), 514–527.
Sorond, F.A., Ratan, R.R., 2000. Ironing-out mechanisms of neuronal injury under hypoxic-ischemic conditions and potential role of iron chelators as neuroprotective agents. Antioxidants & redox signaling 2 (3), 421–436.
Spinu, N., Bal-Price, A., Cronin, M.T.D., Enoch, S.J., Madden, J.C., Worth, A.P., 2019. Development and analysis of an adverse outcome pathway network for human neurotoxicity. Arch. Toxicol. 93 (10), 2759–2772.
Stavenes Andersen, I., Voie, O.A., Fonnum, F., Mariussen, E., 2009. Effects of methyl mercury in combination with polychlorinated biphenyls and brominated flame retardants on the uptake of glutamate in rat brain synaptosomes: a mathematical approach for the study of mixtures. Toxicol. Sci. 112 (1), 175–184.
Stocker, R., 1990. Induction of Heme Oxygenase as a Defense against Oxidative Stress. Free Radical Res Com 9 (2), 101–112.
Suk, K., Kim, S.Y., Kim, H., 2002. Essential role of caspase-11 in activation-induced cell death of rat astrocytes. J Neurochem 80 (2), 230–238.
Swanson, D.A., Steel, J.M., Valle, D., 1998. Identification and characterization of the human ortholog of rat STXBP1, a protein implicated in vesicle trafficking and neurotransmitter release. Genomics 48 (3), 373–376.
Tan, Y., Song, R., Lawrence, D., Carpenter, D.O., 2004. Ortho-substituted but not coplanar PCBs rapidly kill cerebellar granule cells. Toxicol. Sci. 79 (1), 147–156.
Tarnok, K., Czondor, K., Jelitai, M., Czirok, A., Schlett, K., 2008. NMDA receptor NR2B subunit over-expression increases cerebellar granule cell migratory activity. J. Neurochem. 104 (3), 818–829.
Thomas, J.W., Novelli, A., Tao-Cheng, J.H., Henneberry, R., Smith, H.H., Banner, C., 1989. Developmental induction of glutaminase in primary cultures of cerebellar granule cells. Brain Res. Mol. Brain Res. 6 (1), 47–54.
Thomsen, C., Stigum, H., Froshaug, M., Broadwell, S.L., Becher, G., Eggesbo, M., 2010. Determinants of brominated flame retardants in breast milk from a large scale Norwegian study. Environ. Int. 36 (1), 68–74.
Toth, A.B., Terauchi, A., Zhang, L.Y., Johnson-Venkatesh, E.M., Larsen, D.J., Sutton, M. A., Umemori, H., 2013. Synapse maturation by activity-dependent ectodomain shedding of SIRPalpha. Nat. Neurosci. 16 (10), 1417–1425.
Trujillo, M., Ferrer-Sueta, G., Thomson, L., Flohe, L., Radi, R., 2007. Kinetics of peroxiredoxins and their role in the decomposition of peroxynitrite. Subcell Biochem 44, 83–113.
Vale, C., Damgaard, I., Suñol, C., Rodríguez-Farré, E., Schousboe, A., 1998. Cytotoxic action of lindane in cerebellar granule neurons is mediated by interaction with inducible GABA(B) receptors. J. Neurosci. Res. 52 (3), 286–294.
Vallano, M.L., Lambolez, B., Audinat, E., Rossier, J., 1996. Neuronal activity differentially regulates NMDA receptor subunit expression in cerebellar granule cells. J. Neurosci. 16 (2), 631–639.
Vivancos, A.P., Castillo, E.A., Biteau, B., Nicot, C., Ayte, J., Toledano, M.B., Hidalgo, E., 2005. A cysteine-sulfinic acid in peroxiredoxin regulates H2O2-sensing by the antioxidant Pap1 pathway. Proc Natl Acad Sci U S A 102 (25), 8875–8880.
Vizcaino, E., Grimalt, J.O., Fernandez-Somoano, A., Tardon, A., 2014. Transport of persistent organic pollutants across the human placenta. Environ. Int. 65, 107–115.
Vuong, A.M., Yolton, K., Webster, G.M., Sjodin, A., Calafat, A.M., Braun, J.M., Dietrich, K.N., Lanphear, B.P., Chen, A., 2016. Prenatal polybrominated diphenyl ether and perfluoroalkyl substance exposures and executive function in school-age children. Environ. Res. 147, 556–564.
Waghulde, H., Cheng, X., Galla, S., Mell, B., Cai, J., Pruett-Miller, S.M., Vazquez, G., Patterson, A., Vijay Kumar, M., Joe, B., 2018. Attenuation of Microbiotal Dysbiosis and Hypertension in a CRISPR/Cas9 Gene Ablation Rat Model of GPER1. Hypertension (Dallas, Tex. : 1979) 72(5), 1125-1132.
Wang, G.J., Thayer, S.A., 2002. NMDA-induced calcium loads recycle across the mitochondrial inner membrane of hippocampal neurons in culture. J. Neurophysiol. 87 (2), 740–749.
Wang, H., Peng, R.Y., 2016. Basic roles of key molecules connected with NMDAR signaling pathway on regulating learning and memory and synaptic plasticity. Mil Med Res 3 (1), 26.
Wnuk, A., Rzemieniec, J., Litwa, E., Lasoń, W., Krzeptowski, W., Wójtowicz, A.K., Kajta, M., 2016. The Crucial Involvement of Retinoid X Receptors in DDE Neurotoxicity. Neurotox. Res. 29 (1), 155–172.
Wu, H., Yu, W., Meng, F., Mi, J., Peng, J., Liu, J., Zhang, X., Hai, C., Wang, X., 2017a. Polychlorinated biphenyls-153 induces metabolic dysfunction through activation of ROS/NF-κB signaling via downregulation of HNF1b. Redox Biol 12, 300–310.
Wu, J., Chen, Y., Yu, S., Li, L., Zhao, X., Li, Q., Zhao, J., Zhao, Y., 2017b. Neuroprotective effects of sulfiredoxin-1 during cerebral ischemia/reperfusion oxidative stress injury in rats. Brain Res Bull 132, 99–108.
Wyllie, D.J., Livesey, M.R., Hardingham, G.E., 2013. Influence of GluN2 subunit identity on NMDA receptor function. Neuropharmacology 74, 4–17.
Yamakura, T., Shimoji, K., 1999. Subunit- and site-specific pharmacology of the NMDA receptor channel. Prog. Neurobiol. 59 (3), 279–298.
Yamasaki, T., Kawaji, K., Ono, K., Bito, H., Hirano, T., Osumi, N., Kengaku, M., 2001. Pax6 regulates granule cell polarization during parallel fiber formation in the developing cerebellum. Development 128 (16), 3133–3144.
Yeung, J., Ha, T.J., Swanson, D.J., Goldowitz, D., 2016. A Novel and Multivalent Role of Pax6 in Cerebellar Development. J. Neurosci. 36 (35), 9057–9069.
Zeng, Z., Song, B., Xiao, R., Zeng, G., Gong, J., Chen, M., Xu, P., Zhang, P., Shen, M., Yi, H., 2019. Assessing the human health risks of perfluorooctane sulfonate by in vivo and in vitro studies. Environ. Int. 126, 598–610.
Zhang, C., Xu, Q., Xiao, X., Li, W., Kang, Q., Zhang, X., Wang, T., Li, Y., 2018. Prenatal Deltamethrin Exposure-Induced Cognitive Impairment in Offspring Is Ameliorated by Memantine Through NMDAR/BDNF Signaling in Hippocampus. Front. Neurosci. 12, 615.
Zhang, H., Li, F., Yang, Y., Chen, J., Hu, X., 2015. SIRP/CD47 signaling in neurological disorders. Brain Res 1623, 74–80.
Zhang, W., Tian, F., Zheng, J., Li, S., Qiang, M., 2016. Chronic Administration of Benzo (a)pyrene Induces Memory Impairment and Anxiety-Like Behavior and Increases of NR2B DNA Methylation. PLoS One 11 (2) e0149574–e149574.
Zou, W., Chen, C., Zhong, Y., An, J., Zhang, X., Yu, Y., Yu, Z., Fu, J., 2013. PI3K/Akt pathway mediates Nrf2/ARE activation in human L02 hepatocytes exposed to low-concentration HBCDs. Environ Sci Technol 47 (21), 12434–12440.